

Chapter 9: Electromagnetic Waves

9.1 Waves at planar boundaries at normal incidence

9.1.1 Introduction

Chapter 9 treats the propagation of plane waves in vacuum and simple media, at planar boundaries, and in combinations confined between sets of planar boundaries, as in waveguides or cavity resonators. Chapter 10 then discusses how such waves can be generated and received by antennas and antenna arrays.

More specifically, Section 9.1 explains how plane waves are reflected from planar boundaries at normal incidence, and Section 9.2 treats reflection and refraction when the waves are incident at arbitrary angles. Section 9.3 then explains how linear combinations of such waves can satisfy all boundary conditions when they are confined within parallel plates or rectangular cylinders acting as waveguides. By adding planar boundaries at the ends of such waveguides, waves can be trapped at the resonant frequencies of the resulting cavity, as explained in Section 9.4. Sections 9.5 then treat waves in anisotropic, dispersive, and ionized media, respectively.

9.1.2 Introduction to boundary value problems

Section 2.2 showed how uniform plane waves could propagate in any direction with any polarization, and could be superimposed in any combination to yield a total electromagnetic field. The general electromagnetic *boundary value problem* treated in Sections 9.1–4 involves determining exactly which, if any, combination of waves matches any given set of *boundary conditions*, which are the relations between the electric and magnetic fields adjacent to both sides of each boundary. These boundaries can generally be both active and passive, the active boundaries usually being sources. Boundary conditions generally constrain $\bar{\mathbf{E}}$ and/or $\bar{\mathbf{H}}$ for all time on the boundary of the two- or three-dimensional region of interest.

The uniqueness theorem presented in Section 2.8 states that only one solution satisfies all Maxwell's equations if the boundary conditions are sufficient. Therefore we may solve boundary value problems simply by hypothesizing the correct combination of waves and testing it against Maxwell's equations. That is, we leave undetermined the numerical constants that characterize the chosen combination of waves, and then determine which values of those constraints satisfy Maxwell's equations. This strategy eases the challenge of hypothesizing the final answer directly. Moreover, symmetry and other considerations often suggest the nature of the wave combination required by the problem, thus reducing the numbers of unknown constants that must be determined.

The four basic steps for solving boundary value problems are:

- 1) Determine the natural behavior of each homogeneous section of the system in isolation (absent its boundaries).

- 2) Express this natural behavior as the superposition of waves characterized by unknown constants; symmetry and other considerations can minimize the number of waves required. Here our basic building blocks are usually uniform plane waves, but other more compact expansions are typically used if the symmetry of the problem permits, as illustrated in Section 4.5.2 for cylindrical and spherical geometries, Section 7.2.2 for TEM transmission lines, and Section 9.3.1 for waveguide modes.
- 3) Write equations for the boundary conditions that must be satisfied by these sets of superimposed waves, and then solve for the unknown constants.
- 4) Test the resulting solution against any of Maxwell's equations that have not already been imposed.

Variations of this four-step procedure can be used to solve almost any problem by replacing Maxwell's equations with their approximate equivalent for the given problem domain.

9.1.3 Reflection from perfect conductors

One of the simplest examples of a boundary value problem is that of a uniform plane wave in vacuum normally incident upon a planar perfect conductor at $z \geq 0$, as illustrated in Figure 9.1.1(a). Step 1 of the general boundary-problem solution method of Section 9.1.2 is simply to note that electromagnetic fields in the medium can be represented by superimposed uniform plane waves.

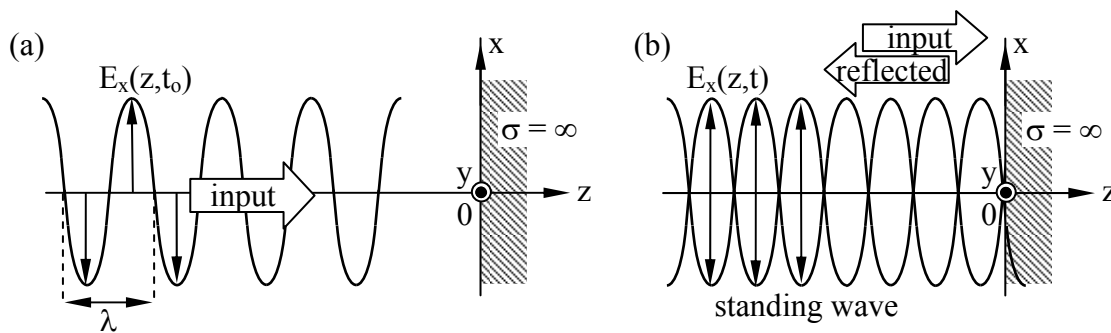


Figure 9.1.1 Plane wave at normal incidence reflecting from a perfect conductor.

For this incompletely defined example, the initial part of Step 2 of the method involves refinement of the problem definition by describing more explicitly the incident wave, for example:

$$\vec{E}(z, t) = \hat{x}E_0 \cos(\omega t - kz) \quad [\text{Vm}^{-1}] \quad (9.1.1)$$

where the wave number $k = 2\pi/\lambda = \omega/c = \omega(\mu_0\epsilon_0)^{0.5}$, (2.3.24). The associated magnetic field (2.3.25) is:

$$\bar{H}(z, t) = \hat{y}(E_o/\eta_o) \cos(\omega t - kz) \quad [\text{Am}^{-1}] \quad (9.1.2)$$

This unambiguously defines the source, and the boundary is similarly unambiguous: $\sigma = \infty$ and therefore $\bar{E} = 0$ for $z \geq 0$. This more complete problem definition is sufficient to yield a unique solution. Often the first step in solving a problem is to ensure its definition is complete.

Since there can be no waves inside the perfect conductor, and since the source field alone does not satisfy the boundary condition $\bar{E}_{//} = 0$ at $z = 0$, one or more additional plane waves must be superimposed to yield a valid solution. In particular, we need to match the boundary condition $\bar{E}_{//} = 0$ at $z = 0$. This can be done by adding a single uniform plane wave propagating in the $-z$ direction with an electric field that cancels the incident electric field at $z = 0$ for all time t . Thus we hypothesize that the total electric field is:

$$\bar{E}(z, t) = \hat{x} [E_o \cos(\omega t - kz) + E_1 \cos(\omega t + kz + \phi)] \quad (9.1.3)$$

where we have introduced the constants E_1 and ϕ .

In Step 3 of the method we must solve the equation (9.1.3) that characterizes the boundary value constraints:

$$\bar{E}(0, t) = \hat{x} [E_o \cos(\omega t - 0) + E_1 \cos(\omega t + 0 + \phi)] = 0 \quad (9.1.4)$$

$$\therefore E_1 = -E_o, \quad \phi = 0 \quad (9.1.5)$$

The result (9.1.5) yields the final trial solution:

$$\bar{E}(z, t) = \hat{x} E_o [\cos(\omega t - kz) - \cos(\omega t + kz)] = \hat{x} 2E_o (\sin \omega t) \sin kz \quad (9.1.6)$$

$$\bar{H}(z, t) = \hat{y} E_o [\cos(\omega t - kz) + \cos(\omega t + kz)] / \eta_o = \hat{y} (2E_o / \eta_o) (\cos \omega t) \cos kz \quad (9.1.7)$$

Note that the sign of the reflected \bar{H} wave is reversed from that of the reflected \bar{E} , consistent with the reversal of the Poynting vector for the reflected wave alone. We have used the identities:

$$\cos \alpha + \cos \beta = 2 \cos [(\alpha + \beta)/2] \cos [(\alpha - \beta)/2] \quad (9.1.8)$$

$$\cos \alpha - \cos \beta = -2 \sin [(\alpha + \beta)/2] \sin [(\alpha - \beta)/2] \quad (9.1.9)$$

Also note that $\bar{H}(z, t)$ is 90° out of phase with $\bar{E}(z, t)$ with respect to both time and space.

We also need a trial solution for $z > 0$. Inside the conductor $\bar{\mathbf{E}} = \bar{\mathbf{H}} = 0$, and boundary conditions (2.6.17) require a surface current:

$$\bar{\mathbf{J}}_s = \hat{n} \times \bar{\mathbf{H}} \quad [\text{m}^{-1}] \quad (9.1.10)$$

The fourth and final step of this problem-solving method is to test the full trial solution against all of Maxwell's equations. We know that our trial solution satisfies the wave equation in our source-free region because our solution is the superposition of waves that do; it therefore also satisfies Faraday's and Ampere's laws in a source-free region, as well as Gauss's laws. At the perfectly conducting boundary we require $\bar{\mathbf{E}}_{//} = 0$ and $\bar{\mathbf{H}}_{\perp} = 0$; these constraints are also satisfied by our trial solution, and therefore the problem is solved for the vacuum. Zero-value fields inside the conductor satisfy all Maxwell's equations, and the surface current $\bar{\mathbf{J}}_s$ (9.1.10) satisfies the final boundary condition.

The nature of this solution is interesting. Note that the total electric field is zero not only at the surface of the conductor, but also at a series of null planes parallel to the conductor and spaced at intervals Δ along the z axis such that $kz_{\text{nulls}} = -n\pi$, where $n = 0, 1, 2, \dots$. That is, the null spacing $\Delta = \pi/k = \lambda/2$, where λ is the wavelength. On the other hand, the magnetic field is maximum at those planes where E is zero (the null planes of E), and has nulls where E is maximum. Since the time average power flow and the Poynting vector are clearly zero at each of these planes, there is no net power flow to the right. Except at the field nulls, however, there is reactive power, as discussed in Section 2.7.3. Because no average power is flowing via these waves and the energy and waves are approximately stationary in space, the solution is called a *standing wave*, as illustrated in Figures 7.2.3 for VSWR and 7.4.1 for resonance on perfectly reflecting TEM transmission lines.

9.1.4 Reflection from transmissive boundaries

Often more than one wave must be added to the given incident wave to satisfy all boundary conditions. For example, assume the same uniform plane wave (9.1.1–2) in vacuum is incident upon the same planar interface, where a medium having $\mu, \epsilon \neq \mu_0, \epsilon_0$ for $z \geq 0$ has replaced the conductor. We have no reason to suspect that the fields beyond the interface are zero, so we might try a trial solution with both a reflected wave $E_r(z, t)$ and a transmitted wave $E_t(z, t)$ having unknown amplitudes (E_r and E_t) and phases (ϕ and θ) for which we can solve:

$$\bar{\mathbf{E}}(z, t) = \hat{x} [E_0 \cos(\omega t - kz) + E_r \cos(\omega t + kz + \phi)] \quad (z < 0) \quad (9.1.11)$$

$$\bar{\mathbf{E}}_t(z, t) = \hat{x} E_t \cos(\omega t - k_t z + \theta) \quad (z \geq 0) \quad (9.1.12)$$

$$\bar{\mathbf{H}}(z, t) = \hat{y} [E_0 \cos(\omega t - kz) - E_r \cos(\omega t + kz + \phi)] / \eta_0 \quad (z < 0) \quad (9.1.13)$$

$$\bar{\mathbf{H}}(z, t) = \hat{y} E_t \cos(\omega t - k_t z + \theta) / \eta_t \quad (z \geq 0) \quad (9.1.14)$$

where $k = \omega\sqrt{\mu_0\epsilon_0}$, $k_t = \omega\sqrt{\mu\epsilon}$, $\eta_0 = \sqrt{\mu_0/\epsilon_0}$, and $\eta_t = \sqrt{\mu/\epsilon}$.

Using these four equations to match boundary conditions at $z = 0$ for $\bar{E}_{//}$ and $\bar{H}_{//}$, both of which are continuous across an insulating boundary, and dividing by E_o , yields:

$$\hat{x}[\cos(\omega t) + (E_r/E_o)\cos(\omega t + \phi)] = \hat{x}(E_t/E_o)\cos(\omega t + \theta) \quad (9.1.15)$$

$$\hat{y}[\cos(\omega t) - (E_r/E_o)\cos(\omega t + \phi)]/\eta_0 = \hat{y}[(E_t/E_o)\cos(\omega t + \theta)]/\eta_t \quad (9.1.16)$$

First we note that for these equations to be satisfied for all time t we must have $\phi = \theta = 0$, unless we reverse the signs of E_r or E_t and let ϕ or $\theta = \pi$, respectively, which is equivalent.

Dividing these two equations by $\cos \omega t$ yields:

$$1 + (E_r/E_o) = E_t/E_o \quad (9.1.17)$$

$$[1 - (E_r/E_o)]/\eta_0 = (E_t/E_o)/\eta_t \quad (9.1.18)$$

These last two equations can easily be solved to yield the *wave reflection coefficient* and the *wave transmission coefficient*:

$$\frac{E_r}{E_o} = \frac{(\eta_t/\eta_0) - 1}{(\eta_t/\eta_0) + 1} \quad (\text{reflection coefficient}) \quad (9.1.19)$$

$$\frac{E_t}{E_o} = \frac{2\eta_t}{\eta_t + \eta_0} \quad (\text{transmission coefficient}) \quad (9.1.20)$$

The wave transmission coefficient E_t/E_o follows from (9.1.17) and (9.1.19). When the characteristic impedance η_t of the dielectric equals that of the incident medium, η_0 , there are no reflections and the transmitted wave equals the incident wave. We then have an *impedance match*. These values for E_r/E_o and E_t/E_o can be substituted into (9.1.11–14) to yield the final solution for $\bar{E}(z, t)$ and $\bar{H}(z, t)$.

The last step of the four-step method for solving boundary value problems involves checking this solution against all Maxwell's equations—they are satisfied.

Example 9.1A

A 1-Wm^{-2} uniform plane wave in vacuum, $\hat{x}E_+ \cos(\omega t - kz)$, is normally incident upon a planar dielectric with $\epsilon = 4\epsilon_0$. What fraction of the incident power P_+ is reflected? What is $\bar{H}(t)$ at the dielectric surface ($z = 0$)?

Solution: $P_-/P_+ = |E_-/E_+|^2 = |(\eta_t - \eta_o)/(\eta_t + \eta_o)|^2$, using (5.1.19). Since $\eta_t = \sqrt{\mu_o/4\epsilon_o} = \eta_o/2$, therefore: $P_-/P_+ = |[(\eta_o/2) - \eta_o]/[(\eta_o/2) + \eta_o]|^2 = (-1/3)^2 = 1/9$. For the forward wave: $\bar{E} = \hat{x}E_+ \cos(\omega t - kz)$ and $\bar{H} = \hat{y}(E_+/\eta_o) \cos(\omega t - kz)$, where $|E_+|^2/2\eta_o = 1$, so $E_+ = (2\eta_o)^{0.5} = (2 \times 377)^{0.5} \cong 27$ [V/m]. The sum of the incident and reflected magnetic fields at $z = 0$ is $\bar{H} = \hat{y}(E_+/\eta_o)[\cos(\omega t) - (1/3)\cos(\omega t)] \cong \hat{y}(27/377)(2/3)\cos(\omega t) = 0.48\hat{y}\cos(\omega t)$ [A m⁻¹]

9.2 Waves incident on planar boundaries at angles

9.2.1 Introduction to waves propagating at angles

To determine electromagnetic fields we can generally solve a boundary value problem using the method of Section 9.1.1, the first step of which involves characterization of the basic quasistatic or dynamic fields and waves that could potentially exist within each separate region of the problem. The final solution is a linear combination of these basic fields and waves that matches all boundary conditions at the interfaces between the various regions.

So far we have considered only waves propagating along boundaries or normal to them. The general case involves waves incident upon boundaries at arbitrary angles, so we seek a compact notation characterizing such waves that simplifies the boundary value equations and their solutions. Because wave behavior at boundaries often becomes frequency dependent, it is convenient to use complex notation as introduced in Section 2.3.2 and reviewed in Appendix B, which can explicitly represent the frequency dependence of wave phenomena. For example, we might represent the electric field associated with a uniform plane wave propagating in the +z direction as $\bar{E}_o e^{-jkz}$, where:

$$\bar{E}(z) = \bar{E}_o e^{-jkz} = \bar{E}_o e^{-j2\pi z/\lambda} \quad (9.2.1)$$

$$\bar{E}_o = \hat{x}E_{ox} + \hat{y}E_{oy} \quad (9.2.2)$$

This notation is simpler than the time domain representation. For example, if this wave were x-polarized, then the compact complex notation $\hat{x}E_x$ would be replaced in the time domain by:

$$\begin{aligned} \bar{E}(t) &= \text{Re} \left\{ \hat{x}E_x(z)e^{j\omega t} \right\} = \hat{x} \text{Re} \left\{ \left(\text{Re}[E_x(z)] + j\text{Im}[E_x(z)] \right) (\cos \omega t + j\sin \omega t) \right\} \\ &= \hat{x} \left\{ \text{Re}[E_x(z)] \cos \omega t - \text{Im}[E_x(z)] \sin \omega t \right\} \end{aligned} \quad (9.2.3)$$

The more general time-domain expression including both x and y components would be twice as long. Thus complex notation adequately characterizes frequency-dependent wave propagation and is more compact.

The physical significance of (9.2.1) is divided into two parts: \bar{E}_0 tells us the polarization, amplitude, and absolute phase of the wave at the origin, and $e^{-j2\pi z/\lambda} \equiv e^{j\phi(z)}$ tells us how the phase ϕ of this wave varies with position. In this case the phase decreases 2π radians as z increases by one wavelength λ . The physical significance of a phase shift ϕ of -2π radians for $z = \lambda$ is that observers located at $z = \lambda$ experience a delay of 2π radians; for pure sinusoids a phase shift of 2π is of course not observable.

Waves propagating in arbitrary directions are therefore easily represented by expressions similar to (9.2.1), but with a phase ϕ that is a function of x, y, and z. For example, a general plane wave would be:

$$\bar{E}(z) = \bar{E}_0 e^{-jk_x x - jk_y y - jk_z z} = \bar{E}_0 e^{-j\bar{k} \cdot \bar{r}} \quad (9.2.4)$$

where $\bar{r} = \hat{x}x + \hat{y}y + \hat{z}z$ and:

$$\bar{k} = \hat{x}k_x + \hat{y}k_y + \hat{z}k_z \quad (9.2.5)$$

We call \bar{k} the *propagation vector* or *wave number* \bar{k} . The wave numbers k_x , k_y , and k_z have the dimensions of radians per meter and determine how rapidly the wave phase ϕ varies with position along the x, y, and z axes, respectively. Positions having the same value for $\bar{k} \cdot \bar{r}$ have the same phase and are located on the same *phase front*. A wave with a planar phase fronts is a *plane wave*, and if its amplitude is constant across any phase front, it is a *uniform plane wave*.

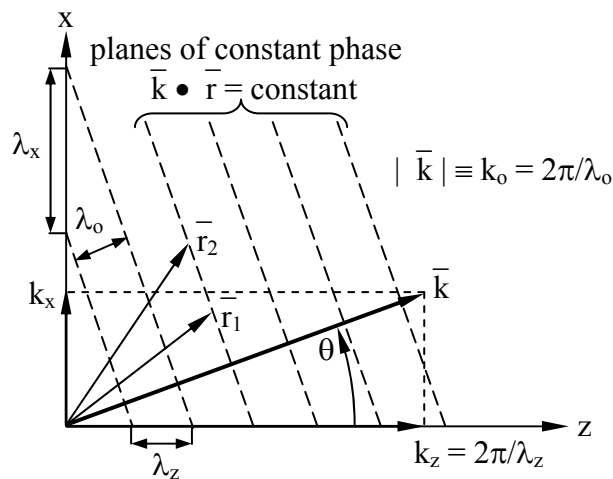


Figure 9.2.1 Uniform plane wave propagating at angle θ in the x-z plane.

The vector \bar{k} points in the direction of propagation for uniform plane waves. The geometry is represented in Figure 9.2.1 for a uniform plane wave propagating in the x-z plane at an angle θ and wavelength λ_0 . The planes of constant phase are perpendicular to the *wave vector* \bar{k} because $\bar{k} \cdot \bar{r}$ must be constant everywhere in such a plane.

The solution (9.2.4) can be substituted into the wave equation (2.3.21):

$$(\nabla^2 + \omega^2 \mu \epsilon) \bar{E} = 0 \quad (9.2.6)$$

This substitution yields⁴⁷:

$$\left[-\left(k_x^2 + k_y^2 + k_z^2\right) + \omega^2 \mu \epsilon \right] \bar{E} = 0 \quad (9.2.7)$$

$$k_x^2 + k_y^2 + k_z^2 = k_0^2 = \omega^2 \mu \epsilon = |\bar{k}|^2 = \bar{k} \cdot \bar{k} \quad (9.2.8)$$

Therefore the figure and (9.2.7) suggest that:

$$k_x = \bar{k} \cdot \hat{x} = k_0 \sin \theta, \quad k_z = \bar{k} \cdot \hat{z} = k_0 \cos \theta \quad (9.2.9)$$

The figure also includes the wave propagation vector components $\hat{x} k_x$ and $\hat{z} k_z$.

Three *projected wavelengths*, λ_x , λ_y , and λ_z , are perceived by observers moving along those three axes. The distance between successive wavefronts at 2π phase intervals is λ_0 in the direction of propagation, and the distances separating these same wavefronts as measured along the x and z axes are equal or greater, as illustrated in Figure 9.2.1. For example:

$$\lambda_z = \lambda_0 / \cos \theta = 2\pi / k_z \geq \lambda_0 \quad (9.2.10)$$

Combining (9.2.8) and (9.2.10) yields:

$$\lambda_x^{-2} + \lambda_y^{-2} + \lambda_z^{-2} = \lambda_0^{-2} \quad (9.2.11)$$

The electric field $\bar{E}(\bar{r})$ for the wave of Figure 9.2.1 propagating in the x-z plane is orthogonal to the wave propagation vector \bar{k} . For simplicity we assume this wave is y-polarized:

$$\bar{E}(\bar{r}) = \hat{y} E_0 e^{-j\bar{k} \cdot \bar{r}} \quad (9.2.12)$$

⁴⁷ $\nabla^2 \bar{E} = \left(\partial^2 / \partial x^2 + \partial^2 / \partial y^2 + \partial^2 / \partial z^2 \right) \bar{E} = -\left(k_x^2 + k_y^2 + k_z^2 \right) \bar{E}$.

The corresponding magnetic field is:

$$\begin{aligned}\bar{\mathbf{H}}(\bar{\mathbf{r}}) &= -(\nabla \times \bar{\mathbf{E}})/j\omega\mu_0 = (\hat{x}\partial\bar{E}_y/\partial z - \hat{z}\partial\bar{E}_y/\partial x)/j\omega\mu_0 \\ &= (\hat{z}\sin\theta - \hat{x}\cos\theta)(E_0/\eta_0)e^{-j\bar{\mathbf{k}}\cdot\bar{\mathbf{r}}}\end{aligned}\quad (9.2.13)$$

One difference between this uniform y-polarized plane wave propagating at an angle and one propagating along a cartesian axis is that $\bar{\mathbf{H}}$ no longer lies along a single axis, although it remains perpendicular to both $\bar{\mathbf{E}}$ and $\bar{\mathbf{k}}$. The next section treats such waves further.

Example 9.2A

If $\lambda_x = 2\lambda_z$ in Figure 9.2.1, what are θ , λ_0 , and $\bar{\mathbf{k}}$?

Solution: By geometry, $\theta = \tan^{-1}(\lambda_z/\lambda_x) = \tan^{-1} 0.5 \cong 27^\circ$. By (9.2.11) $\lambda_0^{-2} = \lambda_x^{-2} + \lambda_z^{-2} = (0.25 + 1)\lambda_z^{-2}$, so $\lambda_0 = 1.25^{-0.5}\lambda_z = 0.89\lambda_z$. $\bar{\mathbf{k}} = \hat{x}k_x + \hat{z}k_z = \hat{x}k_0 \sin\theta + \hat{z}k_0 \cos\theta$, where $k_0 = 2\pi/\lambda_0$. Alternatively, $\bar{\mathbf{k}} = \hat{x}2\pi/\lambda_x + \hat{z}2\pi/\lambda_z$.

9.2.2 Waves at planar dielectric boundaries

Waves at planar dielectric boundaries are solved using the boundary-value-problem method of Section 9.1.4 applied to waves propagating at angles, as introduced in Section 9.2.1.

Because the behavior of waves at an interface depends upon their polarization we need a coordinate system for characterizing it. For this purpose the *plane of incidence* is defined as the plane of projection of the incident wave propagation vector $\bar{\mathbf{k}}$ upon the interface, as illustrated in Figure 9.2.2(a). One cartesian axis is traditionally defined as being normal to this plane of incidence; in the figure it is the y axis.

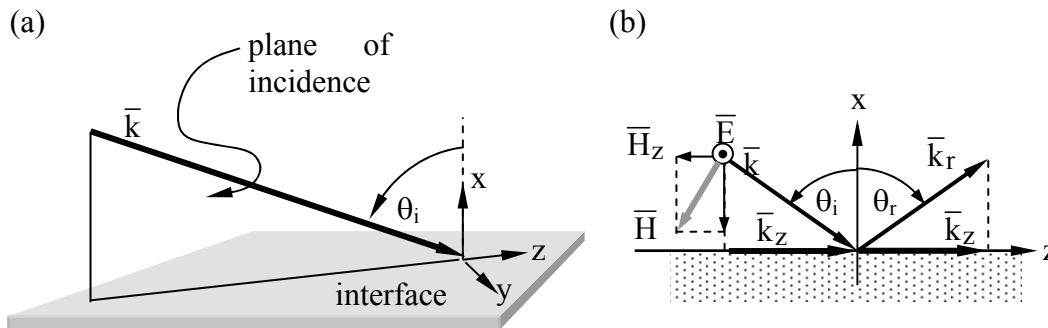


Figure 9.2.2 Uniform plane wave incident upon a planar interface.

We know from Section 2.3.4 that any pair of orthogonally polarized uniform plane waves can be superimposed to achieve any arbitrary wave polarization. For example, x- and y-polarized waves can be superimposed. It is customary to recognize two simple types of incident

electromagnetic waves that can be superimposed to yield any incident wave polarization: *transverse electric waves (TE waves)* are linearly polarized transverse to the plane of incidence (y-polarized in the figure), and *transverse magnetic waves (TM waves)* have the orthogonal linear polarization so that the magnetic field is purely transverse (again if y-polarized). TE and TM waves are typically transmitted and reflected with different amplitudes.

Consider first a TE wave incident upon the planar interface of Figure 9.2.2(b) at the incidence angle θ_i . The corresponding \bar{H} lies in the x-z plane and is orthogonal to \bar{E} . \bar{H} points downward in the figure, corresponding to power $\bar{S} = \bar{E} \times \bar{H}$ propagating toward the interface, where \bar{S} is the Poynting vector for the incident wave. The wavelength of the wave above the interface is $\lambda_o = 1/(f\sqrt{\mu\varepsilon})$ in the medium characterized by permittivity ε and permeability μ . The medium into which the wave is partially transmitted is characterized by ε_t and μ_t , and there the wave has wavelength $\lambda_t = 1/(f\sqrt{\mu_t\varepsilon_t})$ and the same frequency f . This incident TE wave can be characterized by:

$$\bar{E}_i = \hat{y}E_o e^{jk_x x - jk_z z} \quad [\text{m}^{-1}] \quad (9.2.14)$$

$$\bar{H}_i = -(\underline{E}_o/\eta)(\hat{x} \sin \theta_i + \hat{z} \cos \theta_i) e^{jk_x x - jk_z z} \quad [\text{m}^{-1}] \quad (9.2.15)$$

where the characteristic impedance of the incident medium is $\eta = \sqrt{\mu/\varepsilon}$, and \bar{H} is orthogonal to \bar{E} .

The transmitted wave would generally be similar, but with a different η_t , θ_t , E_t , and \bar{k}_t . We might expect a reflected wave as well. The boundary-value-problem method of Section 9.1.2 requires expressions for all waves that might be present in both regions of this problem. In addition to the incident wave we therefore might add general expressions for reflected and transmitted waves having the same TE polarization. If still other waves were needed then no solution satisfying all Maxwell's equations would emerge until they were added too; we shall see no others are needed here. These general reflected and transmitted waves are:

$$\bar{E}_r = \hat{y}E_r e^{-jk_{rx} x - jk_{rz} z} \quad [\text{m}^{-1}] \quad (9.2.16)$$

$$\bar{H}_r = (\underline{E}_r/\eta)(-\hat{x} \sin \theta_r + \hat{z} \cos \theta_r) e^{-jk_{rx} x - jk_{rz} z} \quad [\text{m}^{-1}] \quad (9.2.17)$$

$$\bar{E}_t = \hat{y}E_t e^{jk_{tx} x - jk_{tz} z} \quad [\text{m}^{-1}] \quad (9.2.18)$$

$$\bar{H}_t = -(\underline{E}_t/\eta_t)(\hat{x} \sin \theta_t + \hat{z} \cos \theta_t) e^{jk_{tx} x - jk_{tz} z} \quad [\text{m}^{-1}] \quad (9.2.19)$$

Boundary conditions that must be met everywhere on the non-conducting surface at $x = 0$ include:

$$\bar{\underline{E}}_{i//} + \bar{\underline{E}}_{r//} = \bar{\underline{E}}_{t//} \quad (9.2.20)$$

$$\bar{\underline{H}}_{i//} + \bar{\underline{H}}_{r//} = \bar{\underline{H}}_{t//} \quad (9.2.21)$$

Substituting into (9.2.20) the values of $\bar{\underline{E}}_{//}$ at the boundaries yields:

$$\underline{E}_o e^{-jk_z z} + \underline{E}_r e^{-jk_{rz} z} = \underline{E}_t e^{-jk_{tz} z} \quad (9.2.22)$$

This equation can be satisfied for all values of z only if all exponents are equal. Therefore $e^{-jk_z z}$ can be factored out, simplifying the boundary-condition equations for both $\bar{\underline{E}}_{//}$ and $\bar{\underline{H}}_{//}$:

$$\underline{E}_o + \underline{E}_r = \underline{E}_t \quad (\text{boundary condition for } E_{//}) \quad (9.2.23)$$

$$\frac{\underline{E}_o}{\eta} \cos \theta_i - \frac{\underline{E}_r}{\eta} \cos \theta_r = \frac{\underline{E}_t}{\eta_t} \cos \theta_t \quad (\text{boundary condition for } H_{//}) \quad (9.2.24)$$

Because the exponential terms in (9.2.22) are all equal, it follows that the phases of all three waves must match along the full boundary, and:

$$k_{iz} = k_{rz} = k_{tz} = k_i \sin \theta_i = k_i \sin \theta_r = k_t \sin \theta_t = 2\pi/\lambda_z \quad (9.2.25)$$

This *phase-matching condition* implies that the wavelengths of all three waves in the z direction must equal the same λ_z . It also implies that the *angle of reflection* θ_r equals the *angle of incidence* θ_i , and that the *angle of transmission* θ_t is related to θ_i by *Snell's law*:

$$\frac{\sin \theta_t}{\sin \theta_i} = \frac{k_i}{k_t} = \frac{c_t}{c_i} = \sqrt{\frac{\mu \epsilon}{\mu_t \epsilon_t}} \quad (\text{Snell's law}) \quad (9.2.26)$$

If $\mu = \mu_t$, then the angle of transmission becomes:

$$\theta_t = \sin^{-1} \left(\sin \theta_i \sqrt{\frac{\epsilon}{\epsilon_t}} \right) \quad (9.2.27)$$

These phase-matching constraints, including Snell's law, apply equally to TM waves.

The magnitudes of the reflected and transmitted TE waves can be found by solving the simultaneous equations (9.2.23) and (9.2.24):

$$\underline{E}_r/\underline{E}_o = \Gamma(\theta_i) = \frac{\eta_t \cos \theta_i - \eta \cos \theta_t}{\eta_t \cos \theta_i + \eta \cos \theta_t} = \frac{\eta_n' - 1}{\eta_n' + 1} \quad (9.2.28)$$

$$\underline{E}_t/\underline{E}_o = \underline{T}(\theta_i) = \frac{2\eta_t \cos\theta_i}{\eta_t \cos\theta_i + \eta \cos\theta_t} = \frac{2\eta_n'}{\eta_n' + 1} \quad (9.2.29)$$

where we have defined the normalized angular impedance for TE waves as $\eta_n' \equiv \eta_t \cos\theta_i / (\eta \cos\theta_t)$. The complex angular reflection and transmission coefficients $\underline{\Gamma}$ and \underline{T} for TE waves approach those given by (9.1.19) and (9.1.20) for normal incidence in the limit $\theta_i \rightarrow 0$. The limit of grazing incidence is not so simple, and even the form of the transmitted wave can change markedly if it becomes evanescent, as discussed in the next section. The results for incident TM waves are postponed to Section 9.2.6. Figure 9.2.6(a) plots $|\underline{\Gamma}(\theta)|^2$ for a typical dielectric interface. It is sometimes useful to note that (9.2.28) and (9.2.29) also apply to equivalent TEM lines for which the characteristic impedances of the input and output lines are $\eta_i/\cos\theta_i$ and $\eta_t/\cos\theta_t$, respectively. When TM waves are incident, the corresponding equivalent impedances are $\eta_i \cos\theta_i$ and $\eta_t \cos\theta_t$, respectively.

Example 9.2B

What fraction of the normally incident power ($\theta_i = 0$) is reflected by a single glass camera lens having $\epsilon = 2.25\epsilon_0$? If $\theta_i = 30^\circ$, what is θ_t in the glass?

Solution: At each interface between air and glass, (9.2.28) yields for $\theta_i = 0$: $\underline{\Gamma}_L = (\eta_n' - 1)/(\eta_n' + 1)$, where $\eta_n' = (\eta_{\text{glass}} \cos\theta_i)/(\eta_{\text{air}} \cos\theta_t) = (\epsilon_i/\epsilon_g)^{0.5} = 1/1.5$. Thus $\underline{\Gamma}_L = (1 - 1.5)/(1 + 1.5) = -0.2$, and $|\underline{\Gamma}|^2 = 0.04$, so ~4 percent of the power is reflected from each of the two curved surfaces for each independent lens, or ~8 percent total; these reflections are incoherent so their reflected powers add. Modern lenses have many elements with different permittivities, but coatings on them reduce these reflections, as discussed in Section 7.3.2 for quarter-wave transformers. Snell's law (9.2.26) yields $\theta_t = \sin^{-1}[(\epsilon_i/\epsilon_t)^{0.5} \sin\theta_i] = \sin^{-1}[(1/1.5)(0.5)] = 19.5^\circ$.

9.2.3 Evanescent waves

Figure 9.2.3 suggests why a special form of electromagnetic wave is sometimes required in order to satisfy boundary conditions. Figure 9.2.3(a) illustrates how the required equality of the z components of the incident, reflected, and transmitted wave propagation vectors \bar{k} controls the angles of reflection and transmission, θ_r and θ_t . The radii of the two semi-circles correspond to the magnitudes of \bar{k}_i and \bar{k}_t .

Figure 9.2.3(b) shows that a wave incident at a certain *critical angle* θ_c will produce a transmitted wave propagating parallel to the interface, provided $|\bar{k}_t| < |\bar{k}_i|$. Snell's law (9.2.26) can be evaluated for $\sin\theta_t = 1$ to yield:

$$\theta_c = \sin^{-1}(c_i/c_t) \text{ for } c_i < c_t \quad (\text{critical angle}) \quad (9.2.30)$$

Figure 9.2.3(b) illustrates why phase matching is impossible with uniform plane waves when $\theta > \theta_c$; $k_z > |\bar{k}_t|$. Therefore the λ_z determined by λ and θ_i is less than λ_t , the natural wavelength of the transmission medium at frequency ω . A non-uniform plane wave is then required for phase matching, as discussed below.

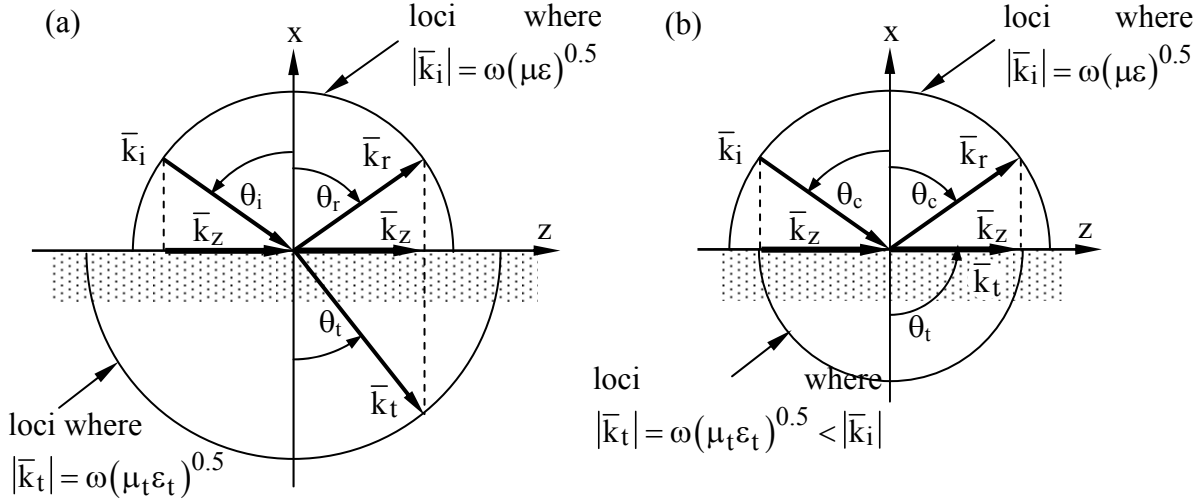


Figure 9.2.3 Angles of reflection and transmission, and the critical angle θ_c .

The wave propagation vector \bar{k}_t must satisfy the wave equation $(\nabla^2 + k_t^2)\underline{\underline{E}} = 0$. Therefore the transmitted wave must be proportional to $e^{-j\bar{k}_t \cdot \bar{r}}$, where $\bar{k}_t = \hat{k}k_t$ and $k_z = k_i \sin \theta_i$, satisfy the expression:

$$k_t^2 = \omega^2 \mu_t \epsilon_t = k_{tx}^2 + k_z^2 \quad (9.2.31)$$

When $k_t^2 < k_z^2$ it follows that:

$$k_{tx} = \pm j(k_z^2 - k_t^2)^{0.5} = \pm j\alpha \quad (9.2.32)$$

We choose the positive sign for α so that the wave amplitude decays with distance from the power source rather than growing exponentially.

The transmitted wave then becomes:

$$\underline{\underline{E}}_t(x, z) = \hat{y} \underline{\underline{E}}_t e^{jk_{tx}x - jk_z z} = \hat{y} \underline{\underline{E}}_t e^{\alpha x - jk_z z} \quad (9.2.33)$$

Note that x is negative in the decay region. The rate of decay $\alpha = (k_i^2 \sin^2 \theta_i - k_t^2)^{0.5}$ is zero when $\theta_i = \theta_c$ and increases as θ_i increases past θ_c ; Waves that decay with distance from an interface and propagate power parallel to it are called *surface waves*.

The associated magnetic field $\bar{\mathbf{H}}_t$ can be found by substituting (9.2.33) into Faraday's law:

$$\bar{\mathbf{H}}_t = \nabla \times \bar{\mathbf{E}} / (-j\omega\mu_t) = -(\bar{\mathbf{E}}_t / \eta_t)(\hat{x} \sin \theta_t - \hat{z} \cos \theta_t) e^{\alpha x - jk_z z} \quad (9.2.34)$$

This is the same expression as (9.2.19), which was obtained for normal incidence, except that the magnetic field and wave now decay with distance x from the interface rather than propagating in that direction. Also, since $\sin \theta_t > 1$ for $\theta_i > \theta_c$, $\cos \theta_t$ is now imaginary and positive, and $\bar{\mathbf{H}}$ is not in phase with $\bar{\mathbf{E}}$. As a result, Poynting's vector for these surface waves has a real part corresponding to real power propagating parallel to the surface, and an imaginary part corresponding to reactive power flowing perpendicular to the surface in the direction of wave decay:

$$\bar{\mathbf{S}} = \bar{\mathbf{E}} \times \bar{\mathbf{H}}^* = (-j\alpha \hat{x} + k_z \hat{z}) (|\bar{\mathbf{E}}_t|^2 / \omega\mu_t) e^{2\alpha x} [\text{Wm}^{-2}] \quad (9.2.35)$$

The reactive part flowing in the $-\hat{x}$ direction is $+j\alpha |\bar{\mathbf{E}}_t|^2 / \omega\mu_t e^{2\alpha x}$ and is therefore inductive (+j), corresponding to an excess of magnetic stored energy relative to electric energy within this surface wave. A wave such as this one that decays in a direction for which the power flow is purely reactive is designated an *evanescent wave*.

An instantaneous view of the electric and magnetic fields of a non-uniform TE plane wave formed at such a dielectric boundary is shown in Figure 9.2.4; these correspond to the fields of (9.2.33) and (9.2.34).

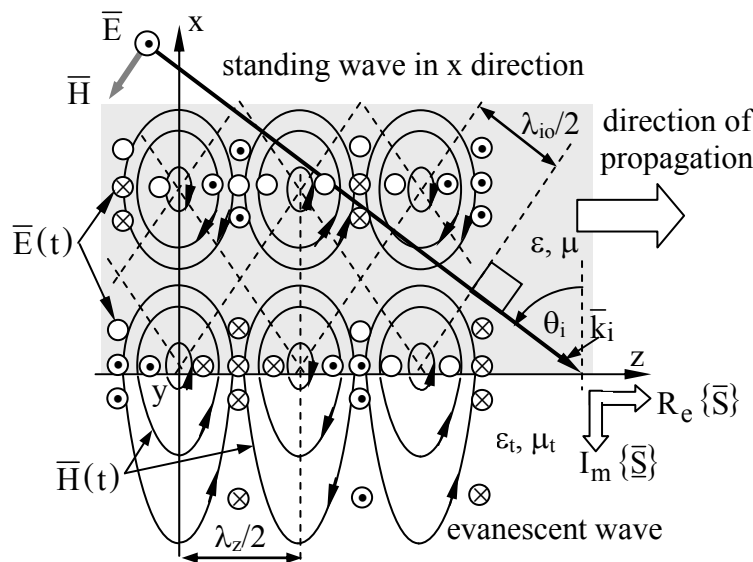


Figure 9.2.4 Evanescent wave traveling in the $+z$ direction at a dielectric interface.

The conventional notation used here indicates field strength by the density of symbols or field lines, and the arrows indicate field direction. Small circles correspond to field lines pointing perpendicular to the page; center dots indicate field lines pointing out of the page in the +y direction and center crosses indicate the opposite, i.e., field lines pointing into the page.

The time average wave intensity in the $+\hat{z}$ direction for x negative and outside the dielectric is:

$$P_z = 0.5R_e \{ \bar{\mathbf{E}} \times \bar{\mathbf{H}}^* \} = (k_z |E_t|^2 / 2\omega\mu_t) e^{\alpha x} [W m^{-2}] \quad (9.2.36)$$

Since the real and imaginary parts of $\bar{\mathbf{S}}$ are orthogonal, there is no decay in the direction of propagation, and therefore no power absorption or heating of the media. Beyond the critical angle θ_c the power is perfectly reflected. In the next section we shall see that the real and imaginary parts of $\bar{\mathbf{S}}$ are often neither orthogonal nor parallel.

9.2.4 Waves in lossy media

Sometimes one or both of the two media are conductive. This section explores the nature of waves propagating in such lossy media having conductivity $\sigma > 0$. Section 9.2.5 then discusses reflections from such media. Losses can also arise if ϵ or μ are complex. The quasistatic relaxation of charge, current, and field distributions in lossy media is discussed separately in Section 4.3.

We can determine the nature of waves in lossy media using the approach of Section 2.3.3 and including the conduction currents $\bar{\mathbf{J}}$ in Ampere's law:

$$\nabla \times \bar{\mathbf{H}} = \bar{\mathbf{J}} + j\omega\epsilon\bar{\mathbf{E}} = \sigma\bar{\mathbf{E}} + j\omega\epsilon\bar{\mathbf{E}} = j\omega\epsilon_{\text{eff}}\bar{\mathbf{E}} \quad (9.2.37)$$

where the effective complex permittivity ϵ_{eff} is:

$$\epsilon_{\text{eff}} = \epsilon [1 - (j\sigma/\omega\epsilon)] \quad (9.2.38)$$

The quantity $\sigma/\omega\epsilon$ is called the *loss tangent* of the medium and indicates how fast waves decay. As we shall see, waves propagate well if $\sigma \ll \omega\epsilon$, and decay rapidly if $\sigma > \omega\epsilon$, sometimes within a fraction of a wavelength.

Substituting ϵ_{eff} for ϵ in $k^2 = \omega^2\mu\epsilon$ yields the dispersion relation:

$$\underline{k}^2 = \omega^2\mu\epsilon [1 - (j\sigma/\omega\epsilon)] = (k' - jk'')^2 \quad (9.2.39)$$

where we define the complex wavenumber \underline{k} in terms of its real and imaginary parts as:

$$\underline{k} = k' - jk'' \quad (9.2.40)$$

The form of the wave solution, following (2.3.26), is therefore:

$$\underline{E}(\underline{r}) = \hat{y}E_0 e^{-jk'z - k''z} \quad [v \text{ m}^{-1}] \quad (9.2.41)$$

This wave has wavelength λ' , frequency ω , and phase velocity v_p inside the conductor related by:

$$k' = 2\pi/\lambda' = \omega/v_p \quad (9.2.42)$$

and the wave decays exponentially with z as $e^{-k''z} = e^{-z/\Delta}$. Note that the wave decays in the same direction as it propagates, corresponding to power dissipation, and that the $1/e$ penetration depth Δ is $1/k''$ meters. Inside conductors, λ' and v_p are much less than their free-space values.

We now need to determine k' and k'' . In general, matching the real and imaginary parts of (9.2.39) yields two equations that can be solved for k' and k'' :

$$(k')^2 - (k'')^2 = \omega^2 \mu \epsilon \quad (9.2.43)$$

$$2k'k'' = \omega \mu \sigma \quad (9.2.44)$$

However, in the limits of very high or very low values of the loss tangent $\sigma/\omega\epsilon$, it is much easier to evaluate (9.2.39) directly.

In the low loss limit where $\sigma \ll \omega\epsilon$, (9.2.39) yields:

$$\underline{k} = \omega \sqrt{\mu \epsilon [1 - (j\sigma/\omega\epsilon)]} \cong \omega \sqrt{\mu \epsilon} - j\sigma\eta/2 \quad (\sigma \ll \omega\epsilon) \quad (9.2.45)$$

where the approximate wave impedance of the medium is $\eta = \sqrt{\mu/\epsilon}$, and we have used the Taylor series approximation $\sqrt{1+\delta} \cong 1 + \delta/2$ for $\delta \ll 1$. In this limit we see from (9.2.45) that λ' and $v_p \cong c$ are approximately the same as they are for the lossless case, and that the $1/e$ penetration depth $\Delta \cong 2/\sigma\eta$, which becomes extremely large as $\sigma \rightarrow 0$.

In the high loss limit where $\sigma \gg \omega\epsilon$, (9.2.39) yields:

$$\underline{k} = \omega \sqrt{\mu \epsilon [1 - (j\sigma/\omega\epsilon)]} \cong \sqrt{-j\mu\omega\sigma} \quad (\sigma \gg \omega\epsilon) \quad (9.2.46)$$

$$\cong \sqrt{\omega\mu\sigma} \sqrt{-j} = \pm \sqrt{\frac{\omega\mu\sigma}{2}} (1-j) \quad (9.2.47)$$

The real and imaginary parts of \underline{k} have the same magnitudes, and the choice of sign determines the direction of propagation. The wave generally decays exponentially as it propagates, although exponential growth occurs in media with negative conductivity. The penetration depth is commonly called the *skin depth* δ in this limit ($\sigma \gg \omega\epsilon$), where:

$$\delta = 1/k'' \cong (2/\omega\mu\sigma)^{0.5} \quad [\text{m}] \quad (\text{skin depth}) \quad (9.2.48)$$

Because the real and imaginary parts of \underline{k} are equal here, both the skin depth and the wavelength λ' inside the conductor are extremely small compared to the free-space wavelength λ ; thus:

$$\lambda' = 2\pi/k' = 2\pi\delta \quad [\text{m}] \quad (\text{wavelength in conductor}) \quad (9.2.49)$$

These distances δ and λ' are extremely short in common metals such as copper ($\sigma \cong 5.8 \times 10^7$, $\mu = \mu_0$) at frequencies such as 1 GHz, where $\delta \cong 2 \times 10^{-6}$ m and $\lambda' \cong 13 \times 10^{-6}$ m, which are roughly five orders of magnitude smaller than the 30-cm free space wavelength. The phase velocity v_p of the wave is reduced by the same large factor.

In the high conductivity limit, the wave impedance of the medium also becomes complex:

$$\underline{\eta} = \sqrt{\frac{\mu}{\epsilon_{\text{eff}}}} = \sqrt{\frac{\mu}{\epsilon(1 - j\sigma/\omega\epsilon)}} \cong \sqrt{\frac{j\omega\mu}{\sigma}} = \sqrt{\frac{\omega\mu}{2\sigma}}(1 + j) \quad (9.2.50)$$

where $+j$ is consistent with a decaying wave in a lossy medium. The imaginary part of $\underline{\eta}$ corresponds to power dissipation, and is non-zero whenever $\sigma \neq 0$.

Often we wish to shield electronics from unwanted external radiation that could introduce noise, or to ensure that no radiation escapes to produce *radio frequency interference* (RFI) that affects other systems. Although the skin depth effect shields electromagnetic radiation, high conductivity will reflect most incident radiation in any event. Conductors generally provide good *shielding* at higher frequencies for which the time intervals are short compared to the magnetic relaxation time (4.3.15) while remaining long compared to the charge relaxation time (4.3.3); Section 4.3.2 and Example 4.3B present examples of magnetic field diffusion into conductors.

Example 9.2C

A uniform plane wave propagates at frequency $f = c/\lambda = 1$ MHz in a medium characterized by ϵ_0 , μ_0 , and conductivity σ . If $\sigma \cong 10^{-3}\omega\epsilon_0$, over what distance D would the wave amplitude decay by a factor of $1/e$? What would be the $1/e$ wave penetration depth δ in a good conductor having $\sigma \cong 10^{11}\omega\epsilon$ at this frequency?

Solution: In the low-loss limit where $\sigma \ll \omega\epsilon$, $\underline{k} \cong \omega/c - j\sigma\eta/2$ (9.2.45), so $E \propto e^{-\sigma\eta z/2} = e^{-z/D}$ where $D = 2/\sigma\eta = 2(\epsilon_0/\mu_0)^{0.5}/10^{-3}\omega\epsilon_0 = 2000c/\omega \cong 318\lambda$ [m]. In the high-loss limit \underline{k}

$\cong (1 \pm j)(\omega\mu\sigma/2)^{0.5}$ so $E \propto e^{-z/\delta}$, where $\delta = (2/\omega\mu\sigma)^{0.5} = (2 \times 10^{-11}/\omega^2\mu\epsilon)^{0.5} = (2 \times 10^{-11})^{0.5}$
 $\lambda/2\pi \cong 7.1 \times 10^{-7}\lambda = 0.21$ mm. This conductivity corresponds to typical metal and the resulting penetration depth is a tiny fraction of a free-space wavelength.

9.2.5 Waves incident upon good conductors

This section focuses primarily on waves propagating inside good conductors. The field distributions produced outside good conductors by the superposition of waves incident upon and reflected from them are discussed in Section 9.2.3.

Section 9.2.4 showed that uniform plane waves in lossy conductors decay as they propagate. The wave propagation constant \underline{k} is then complex in order to characterize exponential decay with distance:

$$\underline{k} = k' - jk'' \quad (9.2.51)$$

The form of a uniform plane wave in lossy media is therefore:

$$\underline{\bar{E}}(\bar{r}) = \hat{y}\underline{E}_0 e^{-jk''z - k'z} \quad [\text{V m}^{-1}] \quad (9.2.52)$$

When a plane wave impacts a conducting surface at an angle, a complex wave propagation vector $\underline{\bar{k}}_t$ is required to represent the resulting transmitted wave. The real and imaginary parts of $\underline{\bar{k}}_t$ are generally at some angle to each other. The result is a *non-uniform plane wave* because its intensity is non-uniform across each phase front.

To illustrate how such transmitted non-uniform plane waves can be found, consider a lossy transmission medium characterized by ϵ , σ , and μ , where we can combine ϵ and σ into a single effective complex permittivity, as done in (9.2.38)⁴⁸:

$$\epsilon_{\text{eff}} \equiv \epsilon(1 - j\sigma/\omega\epsilon) \quad (9.2.53)$$

If we represent the electric field as $\underline{\bar{E}}_0 e^{-j\underline{\bar{k}} \cdot \bar{r}}$ and substitute it into the wave equation $(\nabla^2 + \omega^2\mu\epsilon)\underline{\bar{E}} = 0$, we obtain for non-zero $\underline{\bar{E}}$ the general *dispersion relation* for plane waves in isotropic lossy media:

$$\left[(-j\underline{\bar{k}}) \cdot (-j\underline{\bar{k}}) + \omega^2\mu\epsilon_{\text{eff}} \right] \underline{\bar{E}} = 0 \quad (9.2.54)$$

$$\underline{\bar{k}} \cdot \underline{\bar{k}} = \omega^2\mu\epsilon_{\text{eff}} \quad (\text{dispersion relation}) \quad (9.2.55)$$

⁴⁸ $\nabla \times \underline{\bar{H}} = \underline{\bar{J}} + j\omega\underline{\bar{E}} = \sigma\underline{\bar{E}} + j\omega\underline{\bar{E}} = j\omega\epsilon_{\text{eff}}\underline{\bar{E}}$

Once a plane of incidence such as the x-z plane is defined, this relation has four scalar unknowns—the real and imaginary parts for each of the x and z (in-plane) components of $\bar{\mathbf{k}}$. At a planar boundary there are four such unknowns for each of the reflected and transmitted waves, or a total of eight unknowns. Each of these four components of $\bar{\mathbf{k}}$ (real and imaginary, parallel and perpendicular) must satisfy a boundary condition, yielding four equations. The dispersion relation (9.2.55) has real and imaginary parts for each side of the boundary, thus providing four more equations. The resulting set of eight equations can be solved for the eight unknowns, and generally lead to real and imaginary parts for $\bar{\mathbf{k}}_t$ that are neither parallel nor perpendicular to each other or to the boundary. That is, the real and imaginary parts of $\bar{\mathbf{k}}$ and $\bar{\mathbf{S}}$ can point in four different directions.

It is useful to consider the special case of reflections from planar conductors for which $\sigma \gg \omega\epsilon$. In this limit the solution is simple because the transmitted wave inside the conductor propagates almost perpendicular to the interface, which can be shown as follows. Equation (9.2.47) gave the propagation constant $\underline{\mathbf{k}}$ for a uniform plane wave in a medium with $\sigma \gg \omega\epsilon$:

$$\underline{\mathbf{k}} \cong \pm \sqrt{\frac{\omega\mu\sigma}{2}}(1-j) \quad (9.2.56)$$

The real part of such a $\bar{\mathbf{k}}$ is so large that even for grazing angles of incidence, $\theta_i \cong 90^\circ$, the transmission angle θ_t must be nearly zero in order to match phases, as suggested by Figure 9.2.3(a) in the limit where k_t is orders of magnitude greater than k_i . As a result, the power dissipated in the conductor is essentially the same as for $\theta_i = 0^\circ$, and therefore depends in a simple way on the induced surface current and parallel surface magnetic field $\bar{\mathbf{H}}_{//}$. $\bar{\mathbf{H}}_{//}$ is simply twice that associated with the incident wave alone ($\bar{\mathbf{H}}_{\perp} \cong 0$); essentially all the incident power is reflected so the incident and reflected waves have the same amplitudes and their magnetic fields add.

The power density P_d [W m^{-2}] dissipated by waves traveling in the +z direction in conductors with an interface at $z = 0$ can be found using the Poynting vector:

$$P_d = \frac{1}{2} \text{Re} \left\{ \left(\bar{\mathbf{E}} \times \bar{\mathbf{H}}^* \right) \cdot \hat{\mathbf{z}} \right\} \Big|_{z=0_+} = \text{Re} \left\{ \frac{|\underline{\mathbf{T}}\mathbf{E}_i|^2}{2\underline{\eta}_t} \right\} = \frac{1}{2} \text{Re} \left\{ \frac{1}{\underline{\eta}_t} \right\} \eta_i^2 |\underline{\mathbf{H}}_i \underline{\mathbf{T}}|^2 \quad (9.2.57)$$

The wave impedance $\underline{\eta}_t$ of the conductor ($\sigma \gg \omega\epsilon$) was derived in (9.2.50), and (9.2.29) showed that $\underline{\mathbf{T}} = 2\underline{\eta}'_n / (\underline{\eta}'_n + 1) \cong 2\underline{\eta}'_n$ for TE waves and $\underline{\eta}'_n = \frac{\eta_t \cos \theta_i}{\eta_i \cos \theta_t} \ll 1$:

$$\underline{\eta}_t \cong (\omega\mu_t/2\sigma)^{0.5} (1+j) \quad (9.2.58)$$

$$\underline{\mathbf{T}}_{\text{TE}}(\theta_i) \cong 2\underline{\eta}'_n / (\underline{\eta}'_n + 1) \cong 2\underline{\eta}'_n \cong 2\underline{\eta}_t \cos \theta_t / \eta_i = (2\omega\mu_t\epsilon_i/\mu_i\sigma)^{0.5} (1+j) \cos \theta_i \quad (9.2.59)$$

Therefore (9.2.57), (9.2.58), and (9.2.59) yield:

$$P_d \cong \sqrt{\frac{\sigma}{2\omega\mu_t}} \frac{\mu_i}{\epsilon_i} |\underline{H}_i|^2 \frac{4\omega\mu_t\epsilon_i}{2\mu_i\sigma} = |\underline{H}(z=0)|^2 \sqrt{\frac{\omega\mu}{8\sigma}} \quad [\text{W/m}^2] \quad (9.2.60)$$

A simple way to remember (9.2.60) is to note that it yields the same dissipated power density that would result if the same surface current \bar{J}_s flowed uniformly through a conducting slab having conductivity σ and a thickness equal to the skin depth $\delta = \sqrt{2/\omega\mu\sigma}$:

$$P_d = \frac{\delta}{2} R_e \{ \underline{E} \cdot \underline{J}^* \} = |\underline{J}|^2 \frac{\delta}{2\sigma} = \frac{|\underline{J}_s|^2}{2\sigma\delta} = |\underline{H}(z=0)|^2 \sqrt{\frac{\omega\mu}{8\sigma}} \quad [\text{W/m}^2] \quad (9.2.61)$$

The significance of this result is that it simplifies calculation of power dissipated when waves impact conductors—we need only evaluate the surface magnetic field under the assumption the conductor is perfect, and then use (9.2.61) to compute the power dissipated per square meter.

Example 9.2D

What fraction of the 10-GHz power reflected by a satellite dish antenna is resistively dissipated in the metal if $\sigma = 5 \times 10^7$ Siemens per meter? Assume normal incidence. A wire of diameter D and made of the same metal carries a current I . What is the approximate power dissipated per meter if the skin depth δ at the chosen frequency is much greater than D ? What is this dissipation if $\delta \ll D$?

Solution: The plane wave intensity is $I = \eta_0 |\underline{H}_+|^2 / 2$ [W/m²], and the power absorbed by a good conductor is given by (9.2.61): $P_d \cong |\underline{H}_+|^2 \sqrt{\omega\mu/4\sigma}$, where the magnetic field near a good conductor is twice the incident magnetic field due to the reflected wave. The fractional power absorbed is:

$$P_d/I = 4\sqrt{\omega\mu/\sigma}/\eta_0 = 4\sqrt{\omega\epsilon_0/\sigma} \cong 4(2\pi \cdot 10^{10} \times 8.8 \times 10^{-12} / 5 \times 10^7)^{0.5} = 4.2 \times 10^{-4}. \text{ If}$$

$\delta \gg D$, then a wire dissipates $|\underline{I}|^2 R/2$ watts = $2|\underline{I}|^2/\sigma\pi D^2$ [W/m²]. The magnetic field around a wire is: $\underline{H} = \underline{I}/\pi D$, and if $\delta \ll D$, then the power dissipated per meter is: $\pi D |\underline{H}|^2 \sqrt{\omega\mu/4\sigma} = |\underline{I}|^2 \sqrt{\omega\mu/4\sigma}/\pi D$ [W/m²], where the surface area for dissipation is πD [m²]. Note that the latter dissipation is now increases with the square-root of frequency and is proportional to $1/\sqrt{\sigma}$, not $1/\sigma$.

9.2.6 Duality and TM waves at dielectric boundaries

Transverse magnetic (TM) waves reflect from planar surfaces just as do TE waves, except with different amplitudes as a function of angle. The angles of reflection and transmission are the

same as for TE waves, however, because both TE and TM waves must satisfy the same phase matching boundary condition (9.2.25).

The behavior of TE waves at planar boundaries is characterized by equations (9.2.14) and (9.2.15) for the incident electric and magnetic fields, (9.2.16) and (9.2.17) for the reflected wave, and (9.2.18) and (9.2.19) for the transmitted wave, supplemented by expressions for the complex reflection and transmission coefficients $\underline{\Gamma} = \underline{E}_r/\underline{E}_o$, (9.2.28), and $\underline{T} = \underline{E}_t/\underline{E}_o$, (9.2.29). Although the analogous behavior of TM waves could be derived using the same boundary-value problem solving method used in Section 9.2.2 for TE waves, the principle of *duality* can provide the same solutions with much less effort.

Duality works because Maxwell's equations without charges or currents are duals of themselves. That is, by transforming $\underline{E} \Rightarrow \underline{H}$, $\underline{H} \Rightarrow -\underline{E}$, and $\epsilon \Leftrightarrow \mu$, the set of Maxwell's equations is unchanged:

$$\nabla \times \underline{E} = -\mu \partial \underline{H} / \partial t \quad \rightarrow \quad \nabla \times \underline{H} = \epsilon \partial \underline{E} / \partial t \quad (9.2.62)$$

$$\nabla \times \underline{H} = \epsilon \partial \underline{E} / \partial t \quad \rightarrow \quad -\nabla \times \underline{E} = \mu \partial \underline{H} / \partial t \quad (9.2.63)$$

$$\nabla \bullet \epsilon \underline{E} = 0 \quad \rightarrow \quad \nabla \bullet \mu \underline{H} = 0 \quad (9.2.64)$$

$$\nabla \bullet \mu \underline{H} = 0 \quad \rightarrow \quad \nabla \bullet \epsilon \underline{E} = 0 \quad (9.2.65)$$

The transformed set of equations on the right-hand side of (9.2.62) to (9.2.65) is the same as the original, although sequenced differently. As a result, any solution to Maxwell's equations is also a solution to the dual problem where the variables and boundary conditions are all transformed as indicated above.

The boundary conditions derived in Section 2.6 for a planar interface between two insulating uncharged media are that $\underline{E}_{//}$, $\underline{H}_{//}$, $\mu \underline{H}_{\perp}$, and $\epsilon \underline{E}_{\perp}$ be continuous across the boundary. Since the duality transformation leaves these boundary conditions unchanged, they are dual too. However, duality cannot be used, for example, in the presence of perfect conductors that force $\underline{E}_{//}$ to zero, but not $\underline{H}_{//}$.

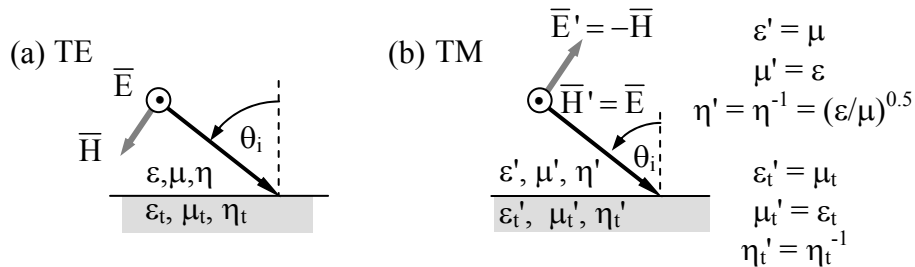


Figure 9.2.5 Dual TE and TM waves incident upon a dual planar boundary.

Figure 9.2.5(b) illustrates a TM plane wave incident upon a planar boundary where both the wave and the boundary conditions are dual to the TE wave illustrated in (a).

The behavior of TM waves at planar boundaries between non-conducting media is therefore characterized by duality transformations of Equations (9.2.62–65) for TE waves, supplemented by similar transformations of the expressions for the complex reflection and transmission coefficients $\underline{\Gamma} = \underline{E}_r/\underline{E}_o$, (9.2.28), and $\underline{T} = \underline{E}_t/\underline{E}_o$, (9.2.29). After the transformations $\underline{E} \Rightarrow \underline{H}$, $\underline{H} \Rightarrow -\underline{E}$, and $\varepsilon \leftrightarrow \mu$, Equations (9.2.14–19) become:

$$\underline{H}_i = \hat{y} \underline{H}_o e^{jk_x x - jk_z z} [\text{Am}^{-1}] \quad (9.2.66)$$

$$\underline{E}_i = (\underline{H}_o \eta) (\hat{x} \sin \theta_i + \hat{z} \cos \theta_i) e^{jk_x x - jk_z z} [\text{Vm}^{-1}] \quad (9.2.67)$$

$$\underline{H}_r = \hat{y} \underline{H}_r e^{-jk_{rx} x - jk_z z} [\text{Am}^{-1}] \quad (9.2.68)$$

$$\underline{E}_r = (\underline{H}_r \eta) (\hat{x} \sin \theta_r - \hat{z} \cos \theta_r) e^{-jk_{rx} x - jk_z z} [\text{Vm}^{-1}] \quad (9.2.69)$$

$$\underline{H}_t = \hat{y} \underline{H}_t e^{jk_{tx} x - jk_z z} [\text{Am}^{-1}] \quad (9.2.70)$$

$$\underline{E}_t = (\underline{H}_t \eta_t) (\hat{x} \sin \theta_t + \hat{z} \cos \theta_t) e^{jk_{tx} x - jk_z z} [\text{Vm}^{-1}] \quad (9.2.71)$$

The complex reflection and transmission coefficients for TM waves are transformed versions of (9.2.28) and (9.2.29), where we define a new angle-dependent η_n by interchanging $\mu \leftrightarrow \varepsilon$ in η_n' in (9.2.28):

$$\underline{H}_r/\underline{H}_o = (\eta_n^{-1} - 1)/(\eta_n^{-1} + 1) \quad (9.2.72)$$

$$\underline{H}_t/\underline{H}_o = 2\eta_n^{-1}/(\eta_n^{-1} + 1) \quad (9.2.73)$$

$$\eta_n^{-1} \equiv \eta \cos \theta_i / (\eta_t \cos \theta_t) \quad (9.2.74)$$

These equations, (9.2.66) to (9.2.74), completely describe the TM case, once phase matching provides θ_r and θ_t .

It is interesting to compare the power reflected for TE and TM waves as a function of the angle of incidence θ_i . Power in uniform plane waves is proportional to both $|\underline{E}|^2$ and $|\underline{H}|^2$. Figure 9.2.6 sketches how the fractional power reflected or *surface reflectivity* varies with angle of incidence θ_i for both TE and TM waves for various impedance mismatches, assuming $\mu = \mu_t$

and $\sigma = 0$ everywhere. If the wave is incident upon a medium with $\epsilon_t > \epsilon$, then $|\Gamma|^2 \rightarrow 1$ as $\theta_i \rightarrow 90^\circ$, whereas $|\Gamma|^2 \rightarrow 1$ at the critical angle θ_c if $\epsilon_t < \epsilon$, and remains unity for $\theta_c < \theta < 90^\circ$ (this θ_c case is not illustrated).

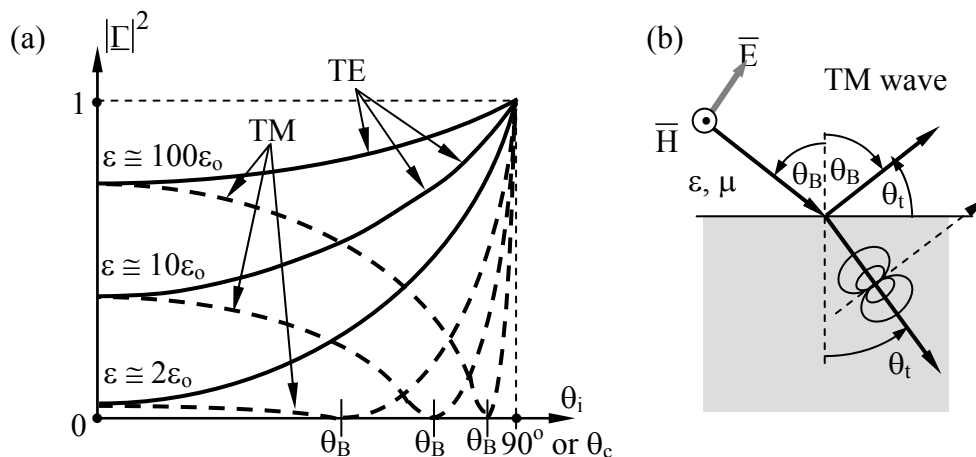


Figure 9.2.6 Power reflected from planar dielectric interfaces for $\mu = \mu_t$.

Figure 9.2.6 reveals an important phenomenon—there is perfect transmission at *Brewster's angle* θ_B for one of the two polarizations. In this case Brewster's angle occurs for the TM polarization because μ is the same everywhere and ϵ is not, and it would occur for TE polarization if μ varied across the boundary while ϵ did not. This phenomenon is widely used in glass *Brewster-angle windows* when even the slightest reflection must be avoided or when pure linear polarization is required (the reflected wave is pure).

We can compute θ_B by noting $\underline{H}_r/\underline{H}_0$ and, using (9.2.72), $\eta_n = 1$. If $\mu = \mu_t$, then (9.2.74) yields $\epsilon_t^{0.5} \cos \theta_i = \epsilon^{0.5} \cos \theta_t$. Snell's law for $\mu = \mu_t$ yields $\epsilon^{0.5} \sin \theta_i = \epsilon_t^{0.5} \sin \theta_t$. These two equations are satisfied if $\sin \theta_i = \cos \theta_t$ and $\cos \theta_i = \sin \theta_t$. Dividing this form of Snell's law by $[\cos \theta_i = \sin \theta_t]$ yields: $\tan \theta_i = (\epsilon_t/\epsilon_i)^{0.5}$, or:

$$\theta_B = \tan^{-1} \sqrt{\epsilon_t/\epsilon_i} \quad (9.2.75)$$

Moreover, dividing $[\sin \theta_i = \cos \theta_t]$ by $[\cos \theta_i = \sin \theta_t]$ yields $\tan \theta_B = \cos \theta_t$, which implies $\theta_B + \theta_t = 90^\circ$. Using this equation it is easy to show that $\theta_B > 45^\circ$ for interfaces where $\theta_t < \theta_i$, and when $\theta_t > \theta_i$, it follows that $\theta_B < 45^\circ$.

One way to physically interpret Brewster's angle for TM waves is to note that at θ_B the polar axes of the electric dipoles induced in the second dielectric ϵ_t are pointed exactly at the angle of reflection mandated by phase matching, but dipoles radiate nothing along their polar axis; Figure 9.2.6(b) illustrates the geometry. That is, $\theta_B + \theta_t = 90^\circ$. For magnetic media

magnetic dipoles are induced, and for TE waves their axes point in the direction of reflection at Brewster's angle.

Yet another way to physically interpret Brewster's angle is to note that perfect transmission can be achieved if the boundary conditions can be matched without invoking a reflected wave. This requires existence of a pair of incidence and transmission angles θ_i and θ_t such that the parallel components of both \vec{E} and \vec{H} for these two waves match across the boundary. Such a pair consistent with Snell's law always exists for TM waves at planar dielectric boundaries, but not for TE waves. Thus there is perfect impedance matching at Brewster's angle.

Example 9.2E

What is Brewster's angle θ_B if $\mu_2 = 4\mu_1$, and $\epsilon_2 = \epsilon_1$, and for which polarization would the phenomenon be observed?

Solution: If the permeabilities differ, but not the permittivities, then Brewster's angle is observed only for TE waves. At Brewster's angle $\theta_B + \theta_t = 90^\circ$, and Snell's law

says $\frac{\sin \theta_t}{\sin \theta_B} = \sqrt{\frac{\mu}{\mu_t}}$. But $\sin \theta_t = \sin(90^\circ - \theta_B) = \cos \theta_B$, so Snell's law becomes:
 $\tan \theta_B = \sqrt{\mu_t/\mu} = 2$, and $\theta_B \cong 63^\circ$.

9.3 Waves guided within Cartesian boundaries

9.3.1 Parallel-plate waveguides

We have seen in Section 9.2 that waves can be reflected at planar interfaces. For example, (9.2.14) and (9.2.16) describe the electric fields for a TE wave reflected from a planar interface at $x = 0$, and are repeated here:

$$\vec{E}_i = \hat{y}E_0 e^{jk_x x - jk_z z} \quad [\text{V m}^{-1}] \quad (\text{incident TE wave}) \quad (9.3.1)$$

$$\vec{E}_r = \hat{y}E_r e^{-jk_x x - jk_z z} \quad (\text{reflected TE wave}) \quad (9.3.2)$$

Note that the subscripts i and r denote "incident" and "reflected", not "imaginary" and "real". These equations satisfy the phase-matching boundary condition that $k_z = k_{zi} = k_{zr}$. Therefore $|k_x|$ is the same for the incident and reflected waves because for both waves $k_x^2 + k_z^2 = \omega^2 \mu \epsilon$.

If the planar interface at $x = 0$ is a perfect conductor, then the total electric field there parallel to the conductor must be zero, implying $\vec{E}_r = -\vec{E}_0$. The superposition of these two incident and reflected waves is:

$$\vec{E}(x, z) = \hat{y}E_0 (e^{jk_x x} - e^{-jk_x x}) e^{-jk_z z} = \hat{y}2jE_0 \sin k_x x e^{-jk_z z} \quad (9.3.3)$$

Thus $\bar{\mathbf{E}} = 0$ in a series of parallel planes located at $x = d$, where:

$$k_x d = n\pi \quad \text{for } n = 0, 1, 2, \dots \quad (\text{guidance condition}) \quad (9.3.4)$$

Because $k_x = 2\pi/\lambda_x$, these planes of electric-field nulls are located at $x_{\text{nulls}} = n\lambda_x/2$. A second perfect conductor could be inserted at any one of these x planes so that the waves would reflect back and forth and propagate together in the $+z$ direction, trapped between the two conducting planes.

We can easily confirm that the boundary conditions are satisfied for the corresponding magnetic field $\bar{\mathbf{H}}(x, z)$ by using Faraday's law:

$$\bar{\mathbf{H}}(x, z) = -(\nabla \times \bar{\mathbf{E}})/j\omega\mu = -(2\mathbf{E}_0/\omega\mu)(\hat{x}jk_z \sin k_x x + \hat{z}k_x \cos k_x x)e^{-jk_z z} \quad (9.3.5)$$

At $x = n\lambda_x/2$ we find $\bar{\mathbf{H}}_{\perp} = \mathbf{H}_x = 0$, so this solution is valid.

Equation (9.3.4), $k_x d = n\pi$ ($n = 1, 2, \dots$), is the *guidance condition* for parallel-plate waveguides that relates mode number to waveguide dimensions; d is the separation of the parallel plates. We can use this guidance condition to make the expressions (9.3.3) and (9.3.5) for $\bar{\mathbf{E}}$ and $\bar{\mathbf{H}}$ more explicit by replacing $k_x x$ with $n\pi x/d$, and k_z with $2\pi/\lambda_z$:

$$\bar{\mathbf{E}}(x, z) = \hat{y}2j\mathbf{E}_0 \sin\left(\frac{n\pi x}{d}\right)e^{-\frac{j2\pi z}{\lambda_z}} \quad (\bar{\mathbf{E}} \text{ for TE}_n \text{ mode}) \quad (9.3.6)$$

$$\bar{\mathbf{H}}(x, z) = -\frac{2\mathbf{E}_0}{\omega\mu} \left[\hat{x}j\frac{2\pi}{\lambda_z} \sin\left(\frac{n\pi x}{d}\right) + \hat{z}\frac{n\pi}{d} \cos\left(\frac{n\pi x}{d}\right) \right] e^{-\frac{j2\pi z}{\lambda_z}} \quad (9.3.7)$$

These electric and magnetic fields correspond to a *waveguide mode* propagating in the $+z$ direction, as illustrated in Figure 9.3.1(a) for a waveguide with plates separated by distance d . The direction of propagation can be inferred from the Poynting vector $\bar{\mathbf{S}} = \bar{\mathbf{E}} \times \bar{\mathbf{H}}^*$. Because this is a TE wave and there is only one half wavelength between the two conducting plates ($n = 1$), this is designated the *TE₁ mode* of a *parallel-plate waveguide*. Because Maxwell's equations are linear, several propagating modes with different values of n can be active simultaneously and be superimposed.

These fields are periodic in both the x and z directions. The wavelength λ_z along the z axis is called the *waveguide wavelength* and is easily found using $k_z = 2\pi/\lambda_z$ where $k^2 = k_x^2 + k_z^2 = \omega^2\mu\epsilon$:

$$\lambda_z = 2\pi(k^2 - k_x^2)^{-0.5} = 2\pi\left[(\omega/c)^2 - (n\pi/d)^2\right]^{-0.5} \quad (\text{waveguide wavelength}) \quad (9.3.8)$$

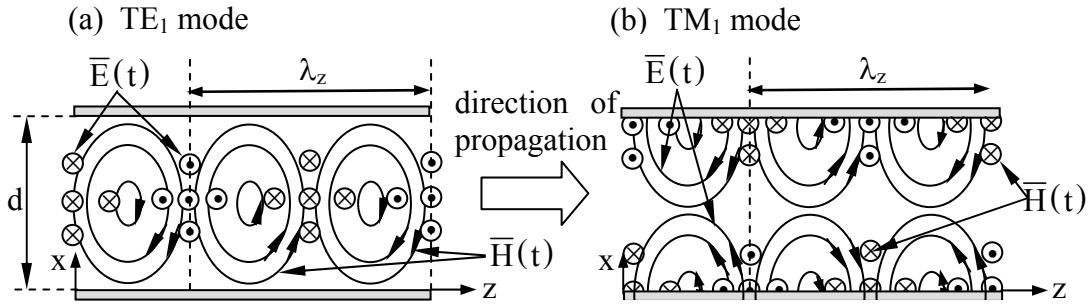


Figure 9.3.1 TE₁ and TM₁ modes of parallel-plate waveguides.

Only those TE_n modes having $n < \omega d/c\pi = 2d/\lambda$ have non-imaginary waveguide wavelengths λ_z and propagate. Propagation ceases when the mode number n increases to the point where $n\pi/d \geq k \equiv 2\pi/\lambda \equiv \omega/c$. This propagation requirement can also be expressed in terms of a minimum frequency ω of propagation, or *cut-off frequency*, for any TE mode:

$$\omega_{TE_n} = n\pi c/d \quad (\text{cut-off frequency for TE}_n \text{ mode}) \quad (9.3.9)$$

Thus each TE_n mode has a minimum frequency ω_{TE_n} for which it can propagate, as illustrated in Figure 9.3.2.

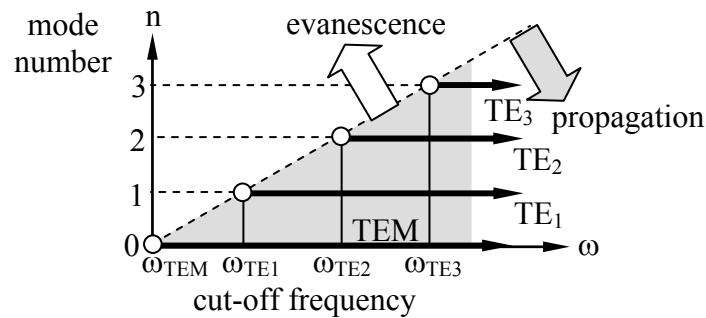


Figure 9.3.2 Propagation frequencies of TE_n modes in parallel-plate waveguides.

The TE₀ mode has zero fields everywhere and therefore does not exist. The TM₀ mode can propagate even DC signals, but is identical to the TEM mode. This same relationship can also be expressed in terms of the maximum free-space wavelength λ_{TE_n} that can propagate:

$$\lambda_{TE_n} = 2d/n \quad (\text{cut-off wavelength } \lambda_{TE_n} \text{ for TE}_n \text{ mode}) \quad (9.3.10)$$

For a non-TEM wave the longest free-space wavelength λ that can propagate in a parallel-plate waveguide of width d is $2d/n$.

If $\omega < \omega_{TE_n}$, then we have an *evanescent wave*; k_z , (9.3.6), and (9.3.7) become:

$$k_z^2 = \omega^2 \mu \epsilon - k_x^2 < 0, \quad k_z = \pm j\alpha \quad (9.3.11)$$

$$\bar{\mathbf{E}}(x, z) = \hat{y} 2jE_0 \sin(n\pi x/d) e^{-\alpha z} \quad (\bar{\mathbf{E}} \text{ for TE}_n \text{ mode, } \omega < \omega_{TE_n}) \quad (9.3.12)$$

$$\bar{\mathbf{H}}(x, z) = -(\nabla \times \bar{\mathbf{E}})/j\omega\mu = -(2E_0/\omega\mu)(\hat{x}\alpha \sin k_x x + \hat{z}k_x \cos k_x x) e^{-\alpha z} \quad (9.3.13)$$

Such evanescent waves propagate no time average power, i.e., $R_e\{\bar{\mathbf{S}}_z\} = 0$, because the electric and magnetic fields are 90 degrees out of phase everywhere and decay exponentially toward zero as z increases, as illustrated in Figure 9.3.3.

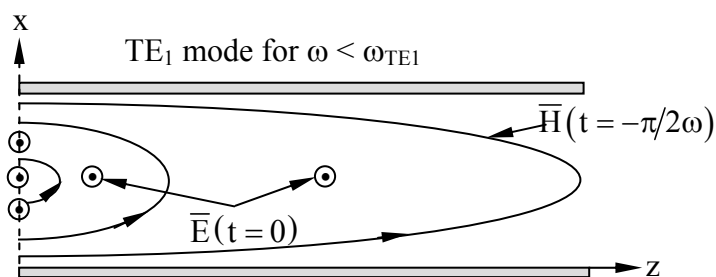


Figure 9.3.3 Evanescent TE₁ mode in a parallel-plate waveguide.

If we reflect a TM wave from a perfect conductor there again will be planar loci where additional perfectly conducting plates could be placed without violating boundary conditions, as suggested in Figure 9.3.1(b) for the TM₁ mode. Note that the field configuration is the same as for the TE₁ mode, except that $\bar{\mathbf{E}}$ and $\bar{\mathbf{H}}$ have been interchanged (allowed by duality) and phase shifted in the lateral direction to match boundary conditions. Between the plates the TE and TM field solutions are dual, as discussed in Section 9.2.6. Also note that TEM = TM₀₁.

Evaluation of Poynting's vector reveals that the waves in Figure 9.3.1 are propagating to the right. If this waveguide mode were superimposed with an equal-strength wave traveling to the left, the resulting field pattern would be similar, but the magnetic and electric field distributions $\bar{\mathbf{E}}(t)$ and $\bar{\mathbf{H}}(t)$ would be shifted relative to one another by $\lambda_z/4$ along the z axis, and they would be 90° out of phase in time; the time-average power flow would be zero, and the reactive power $I_m\{\bar{\mathbf{S}}\}$ would alternate between inductive (+j) and capacitive (-j) at intervals of $\lambda_z/2$ down the waveguide.

Because k_z/ω is frequency dependent, the shapes of waveforms evolve as they propagate. If the signal is narrowband, this evolution can be characterized simply by noting that the envelope of the waveform propagates at the “group velocity” v_g , and the modulated sinusoidal wave inside the envelope propagates at the “phase velocity” v_p , as discussed more fully in Section 9.5.2. These velocities are easily found from $k(\omega)$: $v_p = \omega/k$ and $v_g = (\partial k/\partial \omega)^{-1}$.

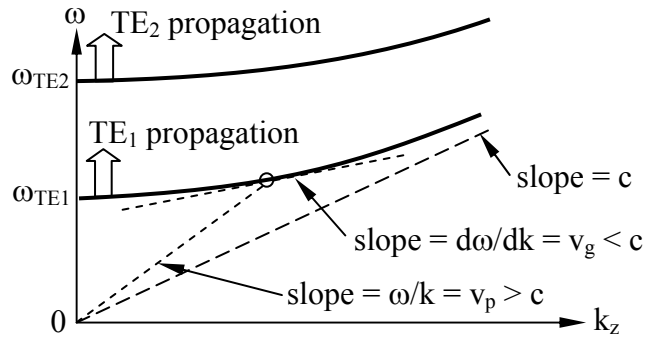


Figure 9.3.4 Dispersion relation and v_p and v_g for a parallel-plate waveguide.

The phase and group velocities of waves in parallel-plate waveguides do not equal c , as can be deduced the dispersion relation plotted in Figure 9.3.4:

$$k_z^2 = \omega^2 \mu \epsilon - k_x^2 = \omega^2 / c^2 - (n\pi/d)^2 \quad (\text{waveguide dispersion relation}) \quad (9.3.14)$$

The phase velocity v_p of a wave, which is the velocity at which the field distribution pictured in Figure 9.3.1 moves to the right, equals ω/k , which approaches infinity as ω approaches the cut-off frequency ω_{TE_n} from above. The group velocity v_g , which is the velocity of energy or information propagation, equals $d\omega/dk$, which is the local slope of the dispersion relation $\omega(k)$ and can never exceed c . Both v_p and v_g approach $c = (\mu\epsilon)^{-0.5}$ as $\omega \rightarrow \infty$.

Example 9.3A

A TM_2 mode is propagating in the $+z$ direction in a parallel-plate waveguide with plate separation d and free-space wavelength λ_o . What are \bar{E} and \bar{H} ? What is λ_z ? What is the decay length α_z^{-1} when the mode is evanescent and $\lambda_o = 2\lambda_{\text{cut off}}$?

Solution: We can superimpose incident and reflected TM waves or use duality to yield $\bar{H}(x,y) = \hat{y} H_o \cos k_x x e^{-jk_z z}$, analogous to (9.3.3), where $k_x d = 2\pi$ for the TM_2 mode. Therefore $k_x = 2\pi/d$ and $k_z = 2\pi/\lambda_z = (k_o^2 - k_x^2)^{0.5} = [(2\pi/\lambda_o)^2 - (2\pi/d)^2]^{0.5}$. Ampere's law yields:

$$\begin{aligned} \bar{E} &= \nabla \times \bar{H} / j\omega\epsilon = (\hat{x} \partial H_y / \partial z + \hat{z} H_y / \partial x) / j\omega\epsilon \\ &= (\hat{x} k_z \cos k_x x + \hat{z} j k_x \sin k_x x) (H_o / \omega\epsilon) e^{-jk_z z} \end{aligned}$$

The waveguide wavelength $\lambda_z = 2\pi/k_z = (\lambda_o^{-2} - d^{-2})^{0.5}$. Cutoff occurs when $k_z = 0$, or $k_o = k_x = 2\pi/d = 2\pi/\lambda_{\text{cut off}}$. Therefore $\lambda_o = 2\lambda_{\text{cut off}} \Rightarrow \lambda_o = 2d$, and $\alpha_o^{-1} = (-jk_z) = (k_x^2 - k_o^2)^{0.5} = [d^{-2} - (2d)^{-2}]^{0.5} / 2\pi = d / (3^{0.5} \pi)$ [m].

9.3.2 Rectangular waveguides

Waves can be trapped within conducting cylinders and propagate along their axis, rectangular and cylindrical waveguides being the most common examples. Consider the *rectangular waveguide* illustrated in Figure 9.3.5. The fields inside it must satisfy the wave equation:

$$(\nabla^2 + \omega^2 \mu \epsilon) \bar{\mathbf{E}} = 0 \quad (\nabla^2 + \omega^2 \mu \epsilon) \bar{\mathbf{H}} = 0 \quad (9.3.15)$$

where $\nabla^2 \equiv \partial^2/\partial x^2 + \partial^2/\partial y^2 + \partial^2/\partial z^2$.

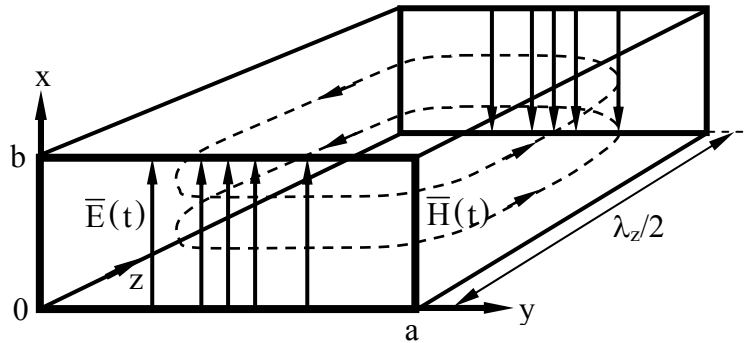


Figure 9.3.5 Dominant mode in rectangular waveguide (TE₁₀).

Since the wave equation requires that the second spatial derivative of $\bar{\mathbf{E}}$ or $\bar{\mathbf{H}}$ equal $\bar{\mathbf{E}}$ or $\bar{\mathbf{H}}$ times a constant, these fields must be products of sinusoids or exponentials along each of the three cartesian coordinates, or sums of such products. For example, the wave equation and boundary conditions ($\bar{\mathbf{E}}_{//} = 0$ at $x = 0$ and $y = 0$) are satisfied by:

$$E_x = \sin k_y y (A \sin k_x x + B \cos k_x x) e^{-jk_z z} \quad (9.3.16)$$

$$E_y = \sin k_x x (C \sin k_y y + D \cos k_y y) e^{-jk_z z} \quad (9.3.17)$$

provided that the usual dispersion relation for uniform media is satisfied:

$$k_x^2 + k_y^2 + k_z^2 = k_0^2 = \omega^2 \mu \epsilon \quad (\text{dispersion relation}) \quad (9.3.18)$$

These field components must also satisfy the boundary condition $\bar{\mathbf{E}}_{//} = 0$ for $x = b$ and $y = a$, which leads to the guidance conditions:

$$k_x b = n\pi \quad (9.3.19)$$

$$k_y a = m\pi \quad (\text{guidance conditions}) \quad (9.3.20)$$

We can already compute the *cut-off frequency* of propagation ω_{mn} for each mode, assuming our conjectured solutions are valid, as shown below. Cut-off occurs when a mode becomes evanescent, i.e., when k_o^2 equals zero or becomes negative. At cut-off for the m,n mode:

$$\omega_{mn}\mu\varepsilon = k_y^2 + k_x^2 = (m\pi/a)^2 + (n\pi/b)^2 \quad (9.3.21)$$

$$\omega_{mn} = \left[(m\pi c/a)^2 + (n\pi c/b)^2 \right]^{0.5} \quad (\text{cut-off frequencies}) \quad (9.3.22)$$

Since $a \geq b$ by definition, and the 0,0 mode cannot have non-zero fields, as shown later, the lowest frequency that can propagate is:

$$\omega_{10} = \pi c/a \quad (9.3.23)$$

which implies that the longest wavelength that can propagate in rectangular waveguide is $\lambda_{\max} = 2\pi c/\omega_{10} = 2a$. If $a > 2b$, the second lowest cut-off frequency is $\omega_{20} = 2\omega_{10}$, so such waveguides can propagate only a single mode over no more than an octave (factor of 2 in frequency) before another propagating mode is added. The parallel-plate waveguides of Section 9.3.1 exhibited similar properties.

Returning to the field solutions, $\bar{\mathbf{E}}$ must also satisfy Gauss's law, $\nabla \cdot \varepsilon \bar{\mathbf{E}} = 0$, within the waveguide, where ε is constant and $E_z \equiv 0$ for TE waves. This implies:

$$\begin{aligned} \nabla \cdot \bar{\mathbf{E}} = 0 = \partial E_x / \partial x + \partial E_y / \partial y + \partial E_z / \partial z = & \left[k_x \sin k_y y (A \cos k_x x \right. \\ & \left. - B \sin k_x x) + k_y \sin k_x x (C \cos k_y y - D \sin k_y y) \right] e^{-jk_z z} \end{aligned} \quad (9.3.24)$$

The only way (9.3.24) can be zero for all combinations of x and y is for:

$$A = C = 0 \quad (9.3.25)$$

$$k_y D = -k_x B \quad (9.3.26)$$

The electric field for TE modes follows from (9.3.17), (9.3.18), (9.3.25), and (9.3.26):

$$\bar{\mathbf{E}} = (\underline{E}_o/k_o) (\hat{x}k_y \sin k_y y \cos k_x x - \hat{y}k_x \sin k_x x \cos k_y y) e^{-jk_z z} \quad (9.3.27)$$

where the factor of k_o^{-1} was introduced so that \underline{E}_o would have its usual units of volts/meter. Note that since $k_x = k_y = 0$ for the TE₀₀ mode, $\bar{\mathbf{E}} = 0$ everywhere and this mode does not exist. The corresponding magnetic field follows from $\bar{\mathbf{H}} = -(\nabla \times \bar{\mathbf{E}})/j\omega\mu$:

$$\begin{aligned}\bar{\mathbf{H}} = & \left(\underline{E}_o / \eta k_o^2 \right) \left(\hat{x} k_x k_z \sin k_x x \cos k_y y + \hat{y} k_y k_z \cos k_x x \sin k_y y \right. \\ & \left. - j \hat{z} k_x^2 \cos k_x x \cos k_y y \right) e^{-jk_z z}\end{aligned}\quad (9.3.28)$$

A similar procedure yields the fields for the TM modes; their form is similar to the TE modes, but with $\bar{\mathbf{E}}$ and $\bar{\mathbf{H}}$ interchanged and then shifted spatially to match boundary conditions. The validity of field solutions where $\bar{\mathbf{E}}$ and $\bar{\mathbf{H}}$ are interchanged also follows from the principle of duality, discussed in Section 9.2.6.

The most widely used rectangular waveguide mode is TE₁₀, often called the *dominant mode*, where the first digit corresponds to the number of half-wavelengths along the wider side of the guide and the second digit applies to the narrower side. For this mode the guidance conditions yield $k_x = 0$ and $k_y = \pi/a$, where $a \geq b$ by convention. Thus the fields (9.3.27) and (9.3.28) become:

$$\bar{\mathbf{E}}_{\text{TE10}} = \underline{E}_o \hat{x} (\sin k_y y) e^{-jk_z z} \quad (\text{dominant mode}) \quad (9.3.29)$$

$$\bar{\mathbf{H}}_{\text{TE10}} = (\underline{E}_o / \omega \mu) \left[\hat{y} k_z \sin(\pi y/a) - j \hat{z} (\pi/a) \cos(\pi y/a) \right] e^{-jk_z z} \quad (9.3.30)$$

The fields for this mode are roughly sketched in Figure 9.3.5 for a wave propagating in the plus- z direction. The electric field varies as the sine across the width a , and is uniform across the height b of the guide; at any instant it also varies sinusoidally along z . H_y varies as the sine of y across the width b , while H_x varies as the cosine; both are uniform in x and vary sinusoidally along z .

The forms of evanescent modes are easily found. For example, the electric and magnetic fields given by (9.3.29) and (9.3.30) still apply even if $k_z = (k_o^2 - k_x^2 - k_y^2)^{0.5} \equiv -j\alpha$ so that $e^{-jk_z z}$ becomes $e^{-\alpha z}$. For frequencies below cutoff the fields for this mode become:

$$\bar{\mathbf{E}}_{\text{TE10}} = \hat{x} \underline{E}_o (\sin k_y y) e^{-\alpha z} \quad (9.3.31)$$

$$\bar{\mathbf{H}}_{\text{TE10}} = -j \left(\pi \underline{E}_o / \eta a k_o^2 \right) \left[\hat{y} \alpha \sin(\pi y/a) + \hat{z} (\pi/a) \cos(\pi y/a) \right] e^{-\alpha z} \quad (9.3.32)$$

The main differences are that for the evanescent wave: 1) the field distribution at the origin simply decays exponentially with distance z and the fields lose their wave character since they wax and wane in synchrony at all positions, 2) the electric and magnetic fields vary 90 degrees out of phase so that the total energy storage alternates twice per cycle between being purely electric and purely magnetic, and 3) the energy flux becomes purely reactive since the real (time average) power flow is zero. The same differences apply to any evanescent TE_{mn} or TM_{mn} mode.

Example 9.3B

What modes have the four lowest cutoff frequencies for a rectangular waveguide having the dimensions $a = 1.2b$? For the TE_{10} mode, where can we cut thin slots in the waveguide walls such that they transect no currents and thus have no deleterious effect?

Solution: The cut-off frequencies (9.3.22) are: $\omega_{mn} = [(m\pi c/a)^2 + (n\pi c/b)^2]^{0.5}$, so the lowest cut-off is for $TE_{mn} = TE_{10}$, since TE_{00} , TM_{00} , TM_{01} , and TM_{10} do not exist. Next comes TE_{11} and TM_{11} , followed by TE_{20} . The wall currents are perpendicular to \bar{H} , which has no x component for the dominant mode (9.3.30); see Figure 9.3.5. Therefore thin slots cut in the x direction in the sidewalls ($y = 0, a$) will never transect current or perturb the TE_{10} mode. In addition, the figure and (9.3.30) show that the z-directed currents at the center of the top and bottom walls are also always zero, so thin z-directed slots at those midlines do not perturb the TE_{10} mode either. Small antennas placed through thin slots or holes in such waveguides are sometimes used to introduce or extract signals.

9.3.3 Excitation of waveguide modes

Energy can be radiated inside waveguides and resonators by antennas. We can compute the energy radiated into each waveguide or resonator mode using modal expansions for the fields and matching the boundary conditions imposed by the given source current distribution \bar{J} .

Consider a waveguide of cross-section $a \times b$ and uniform in the z direction, where $a \geq b$. If we assume the source current \bar{J}_s is confined at $z = 0$ to a wire or current sheet in the x,y plane, then the associated magnetic fields \bar{H}_+ and \bar{H}_- at $z = 0 \pm \delta$, respectively ($\delta \rightarrow 0$), must satisfy the boundary condition (2.1.11):

$$\bar{H}_+ - \bar{H}_- = \bar{J}_s \times \hat{z} \quad (9.3.33)$$

Symmetry dictates $\bar{H}_-(x,y) = -\bar{H}_+(x,y)$ for the x-y components of the fields on the two sides of the boundary at $z = 0$, assuming there are no other sources present, so:

$$\hat{z} \times (\bar{H}_+ - \bar{H}_-) = \hat{z} \times (\bar{J}_s \times \hat{z}) = \bar{J}_s = 2\hat{z} \times \bar{H}_+(x,y) \quad (9.3.34)$$

To illustrate the method we restrict ourselves to the simple case of $TE_{m,0}$ modes, for which \bar{E} and \bar{J}_s are in the x direction. The total magnetic field (9.3.28) summed over all $TE_{m,0}$ modes and orthogonal to \hat{z} for forward propagating waves is:

$$\bar{H}_{+total} = \hat{y} \sum_{m=0}^{\infty} \left[\frac{E_{m,0} m \pi}{(\eta a k_o^2)} \right] k_{zm} \sin(m\pi y/a) = (\bar{J}_s/2) \times \hat{z} \quad (9.3.35)$$

where \underline{E}_m is the complex amplitude of the electric field for the $TE_{m,0}$ mode, and k_y has been replaced by $m\pi/a$. We can multiply both right-hand sides of (9.3.35) by $\sin(n\pi y/a)$ and integrate over the x-y plane to find:

$$\begin{aligned} \sum_{m=0}^{\infty} \left[\underline{E}_{m,0} m\pi / (\eta a k_o^2) \right] k_{zm} \iint_A \sin(m\pi y/a) \sin(n\pi y/a) dx dy \\ = 0.5 \iint_A \underline{J}_s(x,y) \sin(n\pi y/a) dx dy \end{aligned} \quad (9.3.36)$$

Because sine waves of different frequencies are orthogonal when integrated over an integral number of half-wavelengths at each frequency, the integral on the left-hand side is zero unless $m = n$. Therefore we have a simple way to evaluate the phase and magnitude of each excited mode:

$$\underline{E}_{n,0} = \left[\eta k_o^2 / nb\pi k_{zn} \right] \iint_A \underline{J}_s(x,y) \sin(n\pi y/a) dx dy \quad (9.3.37)$$

Not all excited modes propagate real power, however. Modes n with cutoff frequencies above ω are evanescent, so $k_{zn} = [k_o^2 - (n\pi/a)^2]^{0.5}$ is imaginary. The associated magnetic field remains in phase with \underline{J}_s and real, and therefore the power in each evanescent wave is imaginary. Since all modes are orthogonal in space, their powers add; for evanescent modes the imaginary power corresponds to net stored magnetic or electric energy. The reactance at the input to the wires driving the current \underline{J}_s is therefore either capacitive or inductive, depending on whether the total energy stored in the reactive modes is predominantly electric or magnetic, respectively.

A more intuitive way to understand modal excitation is to recognize that the power P delivered to the waveguide by a current distribution \underline{J}_s is:

$$P = \iiint_V \underline{E} \bullet \underline{J}_s^* dv \text{ [V]} \quad (9.3.38)$$

and therefore any mode for which the field distribution \underline{E} is orthogonal to \underline{J}_s will not be excited, and vice versa. For example, a straight wire in the x direction across a waveguide carrying current at some frequency ω will excite all TE_{n0} modes that have non-zero \underline{E} at the position of the wire; modes with cutoff frequencies above ω will contribute only reactance to the current source, while the propagating modes will contribute a real part. Proper design of the current distribution \underline{J}_s can permit any combination of modes to be excited, while not exciting the rest.

9.4 Cavity resonators

9.4.1 Rectangular cavity resonators

Rectangular *cavity resonators* are hollow rectangular conducting boxes of width a , height b , and length d , where $d \geq a \geq b$ by convention. Since they are simply rectangular waveguides terminated at both ends by conducting walls, and the electric fields must still obey the wave equation, $(\nabla^2 + \omega^2\mu\epsilon)\bar{\mathbf{E}} = 0$, therefore $\bar{\mathbf{E}}$ for TE modes must have the form of the TE waveguide fields (9.3.27), but with a sinusoidal z dependence that matches the boundary conditions at $z = 0$ and $z = d$; for example, equal forward- and backward-propagating waves would form the standing wave:

$$\bar{\mathbf{E}} = (\mathbf{E}_0/k_0)(\hat{x}k_y \sin k_y y \cos k_x x - \hat{y}k_x \sin k_x x \cos k_y y)(\underline{A} \sin k_z z + \underline{B} \cos k_z z) \quad (9.4.1)$$

where $B = 0$ ensures $\bar{\mathbf{E}}_{//} = 0$ at $z = 0$, and $k_z = p\pi/d$ ensures it for $z = d$, where $p = 1, 2, \dots$

Unlike rectangular waveguides that propagate any frequency above cut-off for the spatial field distribution (mode) of interest, cavity resonators operate only at specific *resonant frequencies* or combinations of them in order to match all boundary conditions. The *resonant frequencies* ω_{mnp} for a rectangular cavity resonator follow from the dispersion relation:

$$\omega_{mnp}^2 \mu\epsilon = k_y^2 + k_x^2 + k_z^2 = (m\pi/a)^2 + (n\pi/b)^2 + (p\pi/d)^2 \quad (9.4.2)$$

$$\omega_{mnp} = \left[(m\pi c/a)^2 + (n\pi c/b)^2 + (p\pi c/d)^2 \right]^{0.5} \quad [\text{r s}^{-1}] \quad (\text{cavity resonances}) \quad (9.4.3)$$

The *fundamental mode* for a cavity resonator is the lowest frequency mode. Since boundary conditions can not be met unless at least two of the quantum numbers m , n , and p are non-zero, the lowest resonant frequency is associated with the two longest dimensions, d and a . Therefore the lowest resonant frequency is:

$$\omega_{101} = \left[(\pi c/a)^2 + (\pi c/d)^2 \right]^{0.5} \quad [\text{radians/sec}] \quad (\text{lowest resonance}) \quad (9.4.4)$$

Cavity resonators are therefore sometimes filled with dielectrics or magnetic materials to reduce their resonant frequencies by reducing c .

The fields for the fundamental mode of a rectangular cavity resonator, TE_{101} , follow from (9.4.1) and Faraday's law:

$$\bar{\mathbf{E}} = \hat{x}E_0 \sin(\pi y/a) \sin(\pi z/d) \quad (\text{fundamental waveguide mode}) \quad (9.4.5)$$

$$\bar{\mathbf{H}} = j\mathbf{E}_o \left(\pi\omega c^2 / \eta \right) \left[\hat{y} \sin(\pi y/a) \cos(\pi z/d)/d - \hat{z} \cos(\pi y/a) \sin(\pi z/d)/a \right] \quad (9.4.6)$$

The total energy w [J] = $w_e(t) + w_m(t)$ in each mode m,n,p of a cavity resonator can be calculated using (2.7.28) and (2.7.29), and will decay exponentially at a rate that depends on total power dissipation P_d [W] due to losses in the walls and in any insulator filling the cavity interior:

$$w(t) \cong w_o e^{-P_d t/w} = w_o e^{-\omega t/Q} \quad (9.4.7)$$

Wall losses and any dissipation in insulators can be estimated by integrating (9.2.60) and (2.7.30), respectively, over the volume of the cavity resonator. The energy stored, power dissipation, and Q can be quite different for different modes, and are characterized by w_{mnp} , $P_{d,mnp}$, and Q_{mnp} , respectively, as defined by either (3.5.23) or (7.4.43):

$$Q_{mnp} = \omega w_{mnp} / P_{d,mnp} \quad (9.4.8)$$

Example 9.4A

What are the lowest resonant frequency and its Q for a perfectly conducting metallic cavity of dimensions a, b, d if it is filled with a medium characterized by ϵ, μ , and σ . Assume $Q \gg 1$.

Solution: The lowest resonant frequency ω_{101} is given by (9.4.4), where $c = (\mu\epsilon)^{-0.5}$: $\omega_{101} = \pi(\mu\epsilon)^{-0.5}(a^{-2} + d^{-2})^{0.5}$. $Q_{101} = \omega_{101} w_{T101} / P_{d101}$ where the total energy stored w_{T101} is twice the average electric energy stored since the total electric and magnetic energy storages are equal. At each point in the resonator the time-average electric energy density stored is $\langle W_e \rangle = \epsilon |\bar{\mathbf{E}}|^2 / 4$ [J m⁻³] and the time-average power dissipated is $\sigma |\bar{\mathbf{E}}|^2 / 2$, [W m⁻³] so the electric-energy/dissipation density ratio everywhere is $\epsilon/2\sigma$, and thus $w_{T101} / P_{d101} = \epsilon/\sigma$, so $Q_{101} = \pi\epsilon(\mu\epsilon)^{-0.5}(a^{-2} + d^{-2})^{0.5} / \sigma$.

9.4.2 Perturbation of resonator frequencies

Often we would like to tune a resonance to some nearby frequency. This can generally be accomplished by changing the shape of the resonator slightly. Although the relationship between shape and resonant frequency can be evaluated using Maxwell's equations, a simpler and more physical approach is taken here.

The energy stored in a resonator can be regarded as a population of N trapped photons at frequency f bouncing about inside. Since the energy E per photon is hf (1.1.10), the total energy in the resonator is:

$$w_T = Nhf \quad (9.4.9)$$

If we force the walls of a resonator to move slowly toward its new shape, they will move either opposite to the forces imposed by the electromagnetic fields inside, or in the same direction, and thereby do positive or negative work, respectively, on those fields. If we do positive work, then the total electromagnetic energy w_T must increase. Since the number of photons remains constant if the shape change is slow compared to the frequency, positive work on the fields results in increased electromagnetic energy and frequency f . If the resonator walls move in the direction of the applied electromagnetic forces, the externally applied work on the fields is negative and the energy and resonant frequency decrease.

The paradigm above leads to a simple expression for the change in resonant frequency of any resonator due to small physical changes. Consider the case of an air-filled metallic cavity of any shape that is perturbed by pushing in or out the walls slightly in one or more places. The electromagnetic force on a conductor has components associated with both the attractive electric and repulsive magnetic pressures on conductors given by (4.1.15) and (4.1.23), respectively. For sinusoidal waves these pressures are:

$$P_e = -\epsilon_0 |\mathbf{E}_0|^2 / 4 \quad [\text{m}^{-2}] \quad (\text{electric pressure}) \quad (9.4.10)$$

$$P_m = \mu_0 |\mathbf{H}_0|^2 / 4 \quad [\text{m}^{-2}] \quad (\text{magnetic pressure}) \quad (9.4.11)$$

But these pressures, except for the negative sign of P_e (corresponding to attraction), are the electric and magnetic energy densities [J m^{-3}].

The work Δw done in moving the cavity boundary slightly is the pressure $P_{e/m}$ applied, times the area over which it is applied, times the distance moved perpendicular to the boundary. For example, Δw equals the inward electromagnetic pressure (\pm energy density) times the increase in volume added by the moving boundary. But this increase in total stored electromagnetic energy is simply:

$$\Delta w_T = Nh\Delta f = -(P_e + P_m)\Delta v_{\text{volume}} = \Delta w_e - \Delta w_m \quad (9.4.12)$$

The signs for the increases in electric and magnetic energy storage Δw_e and Δw_m and pressures P_e and P_m are different because the pressures P_e and P_m are in opposite directions, where $\Delta w_e = W_e\Delta v_{\text{ol}}$, and $\Delta w_m = -P_m\Delta v_{\text{ol}} = -W_m\Delta v_{\text{ol}}$. Δw_e is defined as the electric energy stored in the increased volume of the cavity, Δv_{ol} , assuming the electric field strength remains constant as the wall moves slightly; Δw_m is defined similarly. The main restriction here is that the walls cannot be moved so far that the force density on the walls changes, nor can their shape change abruptly for the same reason. For example, a sharp point concentrates electric fields and would violate this constraint.

Dividing (9.4.12) by $w_T = Nh f$ yields the frequency perturbation equation:

$$\Delta w_T/w_T = \Delta f/f = (\Delta w_e - \Delta w_m)/w_T = \Delta v_{ol} (W_e - W_m)/w_T \quad (9.4.13)$$

(frequency perturbation)

A simple example illustrates its use. Consider a rectangular cavity resonator operating in the TE₁₀₁ mode with the fields given by (5.4.37) and (5.4.38). If we push in the center of the top or bottom of the cavity where $\bar{H} \cong 0$ and $\bar{E} \neq 0$ we are reducing the volume allocated to electric energy storage, so Δw_e is negative and the resonant frequency will drop in accord with (9.4.13). If we push in the sides, however, the resonant frequency will increase because we are reducing the volume where magnetic energy is stored and Δw_m is negative; the electric energy density at the sidewalls is zero. In physical terms, pushing in the top center where the electric fields pull inward on the wall means that those fields are doing work on the moving wall and therefore lose energy and frequency. Pushing in where the magnetic fields are pushing outward does work on the fields, increasing their energy and frequency. This technique can be used to determine experimentally the unknown resonant mode of a cavity as well as tuning it.

9.5 Waves in complex media

9.5.1 Waves in anisotropic media

There are many types of media that can be analyzed simply using Maxwell's equations, which characterize media by their permittivity ϵ , permeability μ , and conductivity σ . In general ϵ , η , and σ can be complex, frequency dependent, and functions of field direction. They can also be functions of density, temperature, field strength, and other quantities. Moreover they can also couple \bar{E} to \bar{B} , and \bar{H} to \bar{D} . In this section we only treat the special cases of anisotropic media (Section 9.5.1), dispersive media (Section 9.5.2), and plasmas (Section 9.5.3). Lossy media were treated in Sections 9.2.4 and 9.2.5.

Anisotropic media, by definition, have permittivities, permeabilities, and/or conductivities that are functions of field direction. We can generally represent these dependences by 3×3 matrices (tensors), i.e.:

$$\bar{D} = \bar{\epsilon} \bar{E} \quad (9.5.1)$$

$$\bar{B} = \bar{\mu} \bar{H} \quad (9.5.2)$$

$$\bar{J} = \bar{\sigma} \bar{E} \quad (9.5.3)$$

For example, (9.5.1) says:

$$\begin{aligned} D_x &= \epsilon_{xx} E_x + \epsilon_{xy} E_y + \epsilon_{xz} E_z \\ D_y &= \epsilon_{yx} E_x + \epsilon_{yy} E_y + \epsilon_{yz} E_z \\ D_z &= \epsilon_{zx} E_x + \epsilon_{zy} E_y + \epsilon_{zz} E_z \end{aligned} \quad (9.5.4)$$

Most media are symmetric so that $\epsilon_{ij} = \epsilon_{ji}$; in this case the matrix $\bar{\epsilon}$ can always be diagonalized by rotating the coordinate system to define new directions x , y , and z that yield zeros off-axis:

$$\bar{\epsilon} = \begin{pmatrix} \epsilon_x & 0 & 0 \\ 0 & \epsilon_y & 0 \\ 0 & 0 & \epsilon_z \end{pmatrix} \quad (9.5.5)$$

These new axes are called the *principal axes* of the medium. The medium is isotropic if the permittivities of these three axes are equal, *uniaxial* if only two of the three axes are equal, and *biaxial* if all three differ. For example, tetragonal, hexagonal, and rhombohedral crystals are uniaxial, and orthorhombic, monoclinic, and triclinic crystals are biaxial. Most constitutive tensors are symmetric (they equal their own transpose), the most notable exception being permeability tensors for magnetized media like plasmas and ferrites, which are hermetian⁴⁹ and not discussed in this text.

One immediate consequence of anisotropic permittivity and (9.5.4) is that \bar{D} is generally no longer parallel to \bar{E} , as suggested in Figure 9.5.1 for a uniaxial medium. When $\epsilon_{xx} \neq \epsilon_{zz}$, \bar{E} and \bar{D} are parallel only if they lie along one of the principal axes. As explained shortly, this property of uniaxial or biaxial media can be used to convert any wave polarization into any other.

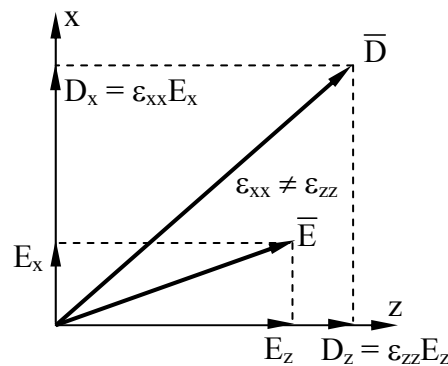


Figure 9.5.1 \bar{D} and \bar{E} in an anisotropic medium.

The origins of anisotropy in media are easy to understand in terms of simple models for crystals. For example, an isotropic cubic lattice becomes uniaxial if it is compressed or stretched along one of those axes, as illustrated in Figure 9.5.2(a) for z -axis compression. That such compressed columns act to increase the effective permittivity in their axial direction can be understood by noting that each of these atomic columns functions like columns of dielectric between capacitor plates, as suggested in Figure 9.5.2(b). Parallel-plate capacitors were

⁴⁹ Hermetian matrices equal the complex conjugate of their transpose.

discussed in Section 3.1.3. Alternatively the same volume of dielectric could be layered over one of the capacitor plates, as illustrated in Figure 9.5.2(c).

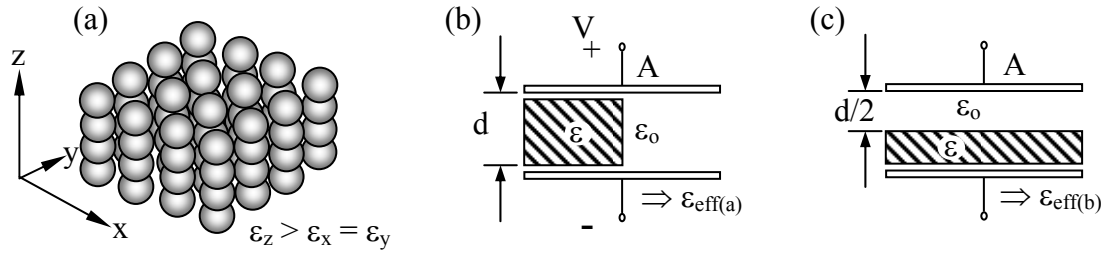


Figure 9.5.2 Uniaxial crystal and anisotropically filled capacitors.

Even though half the volume between the capacitor plates is occupied by dielectric in both these cases, the capacitance for the columns [Figure 9.5.2(b)] is greater, corresponding to a greater effective permittivity ϵ_{eff} . This can be shown using Equation (3.1.10), which says that a parallel plate capacitor has $C = \epsilon_{\text{eff}}A/d$, where A is the plate area and d is the distance between the plates. The capacitances C_a and C_b for Figures 9.5.2(b) and (c) correspond to two capacitors in parallel and series, respectively, where:

$$C_a = (\epsilon A/2d) + (\epsilon_0 A/2d) = (\epsilon + \epsilon_0) A/2d = \epsilon_{\text{eff}(a)} A/d \quad (9.5.6)$$

$$C_b = \left[(\epsilon A/2d)^{-1} + (\epsilon_0 A/2d)^{-1} \right]^{-1} = \left[\epsilon \epsilon_0 / (\epsilon + \epsilon_0) \right] 2A/d = \epsilon_{\text{eff}(b)} A/d \quad (9.5.7)$$

In the limit where $\epsilon \gg \epsilon_0$ the permittivity ratio $\epsilon_{\text{eff}(a)} / \epsilon_{\text{eff}(b)} \rightarrow \epsilon/4\epsilon_0 > 1$. In all compressive cases $\epsilon_{\text{eff}(a)} \geq \epsilon_{\text{eff}(b)}$. If the crystal were stretched rather than compressed, this inequality would be reversed. Exotic complex materials can exhibit inverted behavior, however.

Since the permittivity here interacts directly only with \bar{E} , not \bar{H} , the velocity of propagation $c = 1/\sqrt{\mu\epsilon}$ depends only on the permittivity in the direction of \bar{E} . We therefore expect slower propagation of waves linearly polarized so that \bar{E} is parallel to an axis with higher values of ϵ . We can derive this behavior from the source-free Maxwell's equations and the matrix constitutive relation (9.5.4).

$$\nabla \times \bar{E} = -j\omega\mu\bar{H} \quad (9.5.8)$$

$$\nabla \times \bar{H} = j\omega\bar{D} \quad (9.5.9)$$

$$\nabla \cdot \bar{D} = 0 \quad (9.5.10)$$

$$\nabla \cdot \bar{B} = 0 \quad (9.5.11)$$

Combining the curl of Faraday's law (9.5.8) with Ampere's law (9.5.9), as we did in Section 2.3.3, yields:

$$\nabla \times (\nabla \times \bar{\mathbf{E}}) = \nabla (\nabla \cdot \bar{\mathbf{E}}) - \nabla^2 \bar{\mathbf{E}} = \omega^2 \mu \bar{\mathbf{D}} \quad (9.5.12)$$

We now assume, and later prove, that $\nabla \cdot \bar{\mathbf{E}} = 0$, so (9.5.12) becomes:

$$\nabla^2 \bar{\mathbf{E}} + \omega^2 \mu \bar{\mathbf{D}} = 0 \quad (9.5.13)$$

This expression can be separated into independent equations for each axis. Waves propagating in the z direction are governed by the x and y components of (9.5.13):

$$\left[\left(\frac{\partial^2}{\partial z^2} \right) + \omega^2 \mu \epsilon_x \right] \bar{E}_x = 0 \quad (9.5.14)$$

$$\left[\left(\frac{\partial^2}{\partial z^2} \right) + \omega^2 \mu \epsilon_y \right] \bar{E}_y = 0 \quad (9.5.15)$$

The wave equation (9.5.14) characterizes the propagation of x-polarized waves and (9.5.15) characterizes y-polarized waves; their wave velocities are $(\mu \epsilon_x)^{-0.5}$ and $(\mu \epsilon_y)^{-0.5}$, respectively. If $\epsilon_x \neq \epsilon_y$ then the axis with the lower velocity is called the "slow" axis, and the other is the "fast" axis. This dual-velocity phenomenon is called *birefringence*. That our assumption $\nabla \cdot \bar{\mathbf{E}} = 0$ is correct is easily seen by noting that the standard wave solution for both x- and y- polarized waves satisfies these constraints. Since ∇ is distributive, the equation is also satisfied for arbitrary linear combinations of x- and y- polarized waves, which is the most general case here.

If a wave has both x- and y-polarized components, the polarization of their superposition will evolve as they propagate along the z axis at different velocities. For example, a linearly wave polarized at 45 degrees to the x and y axes will evolve into elliptical and then circular polarization before evolving back into linear polarization orthogonal to the input.

This ability of a birefringent medium to transform polarization is illustrated in Figure 9.5.3. In this case we can represent the linearly polarized wave at $z = 0$ as:

$$\bar{\mathbf{E}}(z = 0) = E_0 (\hat{x} + \hat{y}) \quad (9.5.16)$$

If the wave numbers for the x and y axes are k_x and k_y , respectively, then the wave at position z will be:

$$\bar{\mathbf{E}}(z) = E_0 e^{-jk_x z} (\hat{x} + \hat{y} e^{j(k_x - k_y)z}) \quad (9.5.17)$$

The phase difference between the x- and y-polarized components of the electric field is therefore $\Delta\phi = (k_x - k_y)z$. As suggested in the figure, circular polarization results when the two

components are 90 degrees out of phase ($\Delta\phi = \pm 90^\circ$), and the orthogonal linear polarization results when $\Delta\phi = 180^\circ$.

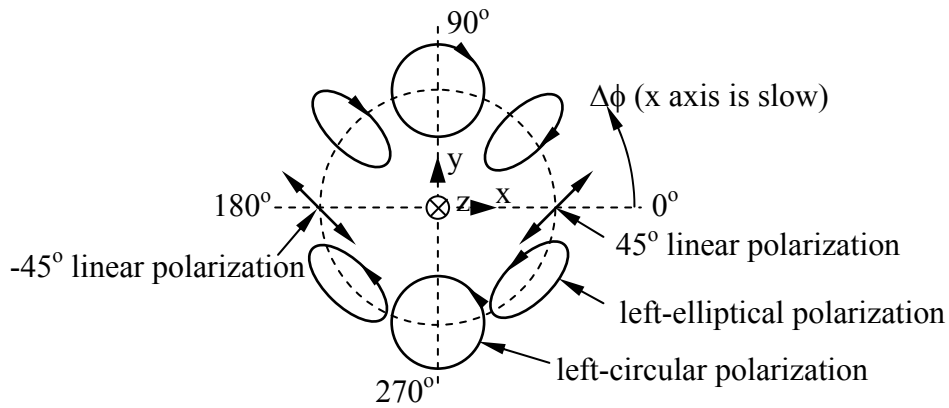


Figure 9.5.3 Polarization conversion in a birefringent medium.

Polarization conversion is commonly used in optical systems to convert linear polarization to circular, or vice-versa, via a *quarter-wave plate* for which $\Delta\phi$ is 90° , equivalent to a quarter wavelength. A *half-wave plate* ($\Delta\phi = 180^\circ$) reverses the sense of any polarization.

Example 9.5A

A certain birefringent medium is characterized by $\mu_o, \epsilon_x = 2\epsilon_o, \epsilon_y = 2.002\epsilon_o$. How thick D must a quarter-wave plate be if $\lambda = 5 \times 10^{-7}$ [m] in free space (visible light)? At what thickness D' might this same plate rotate appropriate linear polarization 90 degrees?

Solution: The phase lags along the x and y axes arise from $e^{-jk_x D}$ and $e^{-jk_y D}$, respectively, and the difference is $\pi/2 = (k_y - k_x)D$ for a quarter-wave plate. But $k_i = \omega(\mu_o \epsilon_i)^{0.5}$, so $(k_y - k_x)D = \omega(\mu_o \epsilon_x)^{0.5} [(1 + 1.001)^{0.5} - 1] D \cong (\omega/c_x)^{0.5} 0.0005 D = \pi/2$. Since $\omega/c_x = 2\pi/\lambda_x$, therefore $D = 2000\lambda_x/4$ where $\lambda_x = 5 \times 10^{-7} (\epsilon_o/\epsilon_x)^{0.5}$. Thus $D = 500\lambda_x = 0.18$ mm, which is approximately the thickness of a Vu-Graph transparency that acts as a quarter-wave plate. A differential phase lag of π yields 90° polarization rotation for waves linearly polarized at an angle 45° from the principal axes x and y , so the thickness would be doubled to ~ 0.36 mm.

9.5.2 Waves in dispersive media

Dispersive media have wave velocities that are frequency dependent due to the frequency dependence of μ, ϵ , or σ . These frequency dependencies arise in all materials because of the non-instantaneous physical responses of electrons to fields. Often these time lags are so brief that only at optical frequencies do they become a significant fraction of a period, although propagation over sufficiently long paths can introduce significant cumulative differences in effects across any frequency band or gap. Only vacuum is essentially non-dispersive.

The principal consequence of dispersion is that narrowband pulse signals exhibit two velocities, the *phase velocity* v_p of the sinusoids within the pulse envelope, and the *group velocity* v_g at which the pulse envelope, energy, and information propagate. Because energy and information travel at the group velocity, it never exceeds the velocity of light although phase velocity frequently does.

A simple way to reveal this phenomenon is to superimpose two otherwise identical sinusoidal waves propagating at slightly different frequencies, $\omega \pm \Delta\omega$; superposition is valid because Maxwell's equations are linear. The corresponding wave numbers are $k \pm \Delta k$, where $\Delta k \ll k$ and $\Delta\omega \ll \omega$. Such a superposition for two sinusoids propagating in the $+z$ direction is:

$$\begin{aligned} E(t, z) &= E_0 \cos[(\omega + \Delta\omega)t - (k + \Delta k)z] + E_0 \cos[(\omega - \Delta\omega)t - (k - \Delta k)z] \\ &= E_0 2 \cos(\omega t - kz) \cos(\Delta\omega t - \Delta k z) \end{aligned} \quad (9.5.18)$$

where we used the identity $\cos \alpha + \cos \beta = 2 \cos[(\alpha + \beta)/2] \cos[(\alpha - \beta)/2]$. The first factor on the right-hand side of (9.5.18) is a sine wave propagating at the center frequency ω at the phase velocity:

$$v_p = \omega/k \quad (\text{phase velocity}) \quad (9.5.19)$$

The second factor is the low-frequency, long-wavelength modulation envelope that propagates at the group velocity $v_g = \Delta\omega/\Delta k$, which is the slope of the $\omega(k)$ *dispersion relation*:

$$v_g = \partial\omega/\partial k = (\partial k/\partial\omega)^{-1} \quad (\text{group velocity}) \quad (9.5.20)$$

Figure 9.5.4(a) illustrates the original sinusoids plus their superposition at two points in time, and Figure 9.5.4(b) illustrates the corresponding dispersion relation.

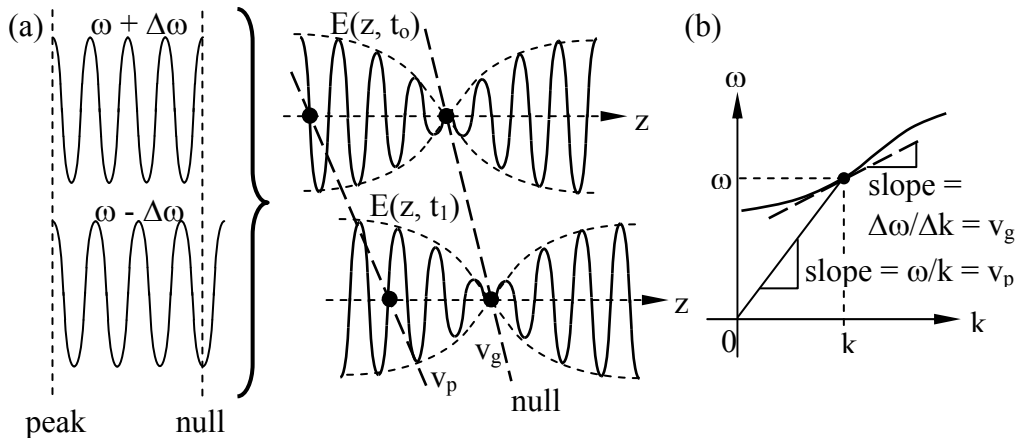


Figure 9.5.4 Phase and group velocity for two superimposed sinusoids.

Note that this dispersion relation has a phase velocity that approaches infinity at the lowest frequencies, which is what happens in plasmas near the plasma frequency, as discussed in the next section.

Communications systems employ finite-duration pulses with Fourier components at all frequencies, so if such pulses travel sufficiently far even the envelope with its finite bandwidth will become distorted. As a result dispersive media are either avoided or compensated in most communications system unless the bandwidths are sufficiently narrow. Compensation is possible because dispersion is a linear process so inverse filters are readily designed. Section 12.2.2 discusses dispersion further in the context of optical fibers.

Example 9.5B

When $\omega = c_0^{0.5}$, what are the phase and group velocities v_p and v_g in a medium having the dispersion relation $k = \omega^2/c_0$?

Solution: $v_p = \omega/k = c_0/\omega = c_0^{0.5}$ [m s⁻¹]. $v_g = (\partial k/\partial \omega)^{-1} = c_0/2\omega = c_0^{0.5}/2$ [m s⁻¹].

9.5.3 Waves in plasmas

A *plasma* is a charge-neutral gaseous assembly of atoms or molecules with enough free electrons to significantly influence wave propagation. Examples include the ionosphere⁵⁰, the sun, interiors of fluorescent bulbs or nuclear fusion reactors, and even electrons in metals or electron pairs in superconductors. We can characterize fields in plasmas once we know their permittivity ϵ at the frequency of interest.

To compute the permittivity of a non-magnetized plasma we recall (2.5.8) and (2.5.13):

$$\bar{D} = \epsilon \bar{E} = \epsilon_0 \bar{E} + \bar{P} = \epsilon_0 \bar{E} + nq\bar{d} \quad (9.5.21)$$

where $q = -e$ is the electron charge, \bar{d} is the mean field-induced displacement of the electrons from their equilibrium positions, and n_3 is the number of electrons per cubic meter. Although positive ions are also displaced, these displacements are generally negligible in comparison to those of the electrons because the electron masses m_e are so much less. We can take the mass m_i of the ions into account simply by replacing m_e in the equations by m_r , the reduced mass of the electrons, where it can be shown that $m_r = m_e m_i / (m_e + m_i) \cong m_e$.

To determine ϵ in (9.5.21) for a collisionless plasma, we merely need to solve Newton's law for $\bar{d}(t)$, where the force \bar{f} follows from (1.2.1):

$$\bar{f} = q\bar{E} = m\bar{a} = m(j\omega)^2 \bar{d} \quad (9.5.22)$$

⁵⁰ The terrestrial ionosphere is a partially ionized layer at altitudes ~50-5000 km, depending primarily upon solar ionization. Its peak electron density is $\sim 10^{12}$ electrons m⁻³ at 100-300 km during daylight.

Solving (9.5.22) for \bar{d} and substituting it into the expression for \bar{P} yields:

$$\bar{P} = nq\bar{d} = -ne\bar{d} = \bar{E}ne^2m^{-1}(j\omega)^{-2} \quad (9.5.23)$$

Combining (9.5.21) and (9.5.23) yields:

$$\bar{D} = \epsilon_0\bar{E} + \bar{P} = \epsilon_0\left[1 + ne^2/m(j\omega)^2\epsilon_0\right]\bar{E} = \epsilon_0\left[1 - \omega_p^2/\omega^2\right]\bar{E} = \epsilon\bar{E} \quad (9.5.24)$$

where ω_p is defined as the *plasma frequency*:

$$\omega_p \equiv (ne^2/m\epsilon_0)^{0.5} \quad [\text{radians s}^{-1}] \quad (9.5.25)$$

The plasma frequency is the natural frequency of oscillation of a displaced electron or cluster of electrons about their equilibrium location in a neutral plasma, and we shall see that the propagation of waves above and below this frequency is markedly different.

The dispersion relation for a collisionless non-magnetic plasma is thus:

$$k^2 = \omega^2\mu\epsilon = \omega^2\mu_0\epsilon_0\left(1 - \omega_p^2/\omega^2\right) \quad (9.5.26)$$

which is plotted as $\omega(k)$ in Figure 9.5.5 together with the slopes representing the phase and group velocities of waves in plasmas.

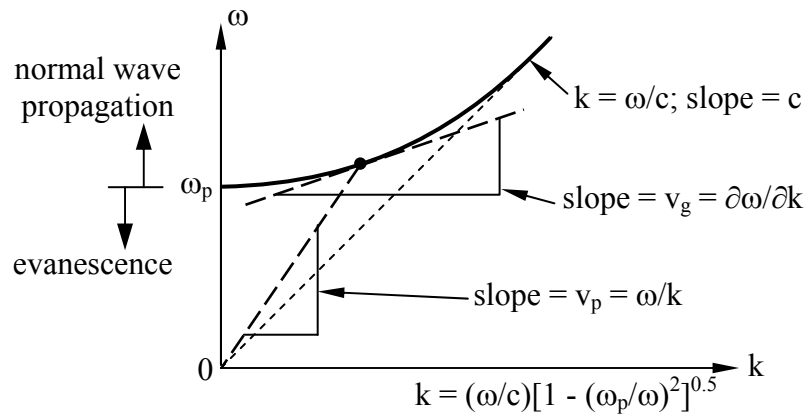


Figure 9.5.5 Dispersion relation and velocities for a simple plasma.

Using the expressions (9.5.19) and (9.5.20) for phase and group velocity we find for plasmas:

$$v_p = \omega/k = c\left[1 - (\omega_p/\omega)^2\right]^{-0.5} \quad (9.5.27)$$

$$v_g = (\partial k / \partial \omega)^{-1} = c \left[1 - (\omega_p / \omega)^2 \right]^{0.5} \quad (9.5.28)$$

Since $v_p v_g = c^2$, and since $v_g \leq c$, it follows that v_p is always equal to or greater than c . However, for $\omega < \omega_p$ we find v_p and v_g become imaginary because normal wave propagation is replaced by another behavior.

From (9.5.26) we see that when $\omega < \omega_p$:

$$\underline{k} = \frac{\omega}{c} \sqrt{1 - (\omega_p / \omega)^2} = \pm j\alpha \quad (9.5.29)$$

$$\underline{\eta} = \sqrt{\frac{\mu}{\epsilon}} = \eta_0 / \sqrt{1 - (\omega_p / \omega)^2} = \mp j \frac{\mu_0 \omega}{\alpha} \quad (9.5.30)$$

Therefore an x-polarized wave propagating in the +z direction would be:

$$\underline{\bar{E}} = \hat{x} E_0 e^{-\alpha z} \quad (9.5.31)$$

$$\underline{\bar{H}} = \hat{y} \underline{\eta}^{-1} E_0 e^{-\alpha z} = j \hat{y} (\alpha / \omega \mu_0) E_0 e^{-\alpha z} \quad (9.5.32)$$

where the sign of $\pm j\alpha$ was chosen (-) to correspond to exponential decay of the wave rather than growth. We find from (9.5.32) that $\underline{\bar{H}}(t)$ is delayed 90° behind $\underline{\bar{E}}(t)$, that both decay exponentially with z , and that the Poynting vector $\underline{\bar{S}}$ is purely imaginary:

$$\underline{\bar{S}} = \underline{\bar{E}} \times \underline{\bar{H}}^* = -j \hat{z} (\alpha |E_0|^2 / \omega \mu_0) e^{-2\alpha z} \quad (9.5.33)$$

Such an *evanescent wave* decays exponentially and carry only reactive power and no time-average power because of the time orthogonality of $\underline{\bar{E}}$ and $\underline{\bar{H}}$. Reactive power implies that below ω_p the average energy stored is predominantly electric, but in this case the stored energy is actually dominated by the kinetic energy of the electrons. It is this extra energy that allows the permittivity ϵ to become negative below ω_p although μ_0 remains constant. The frequency ω_p below which conversion from propagation to evanescence occurs is called the *cut-off frequency*, which is the plasma frequency here.

Example 9.5C

What is the plasma frequency f_p [Hz] of the ionosphere when $n_e = 10^{12} \text{ m}^{-3}$?

Solution: $f_p = \omega_p / 2\pi = (10^{12} e^2 / m \epsilon_0)^{0.5} / 2\pi \cong 9.0 \text{ MHz}$.

MIT OpenCourseWare
<http://ocw.mit.edu>

6.013 Electromagnetics and Applications
Spring 2009

For information about citing these materials or our Terms of Use, visit: <http://ocw.mit.edu/terms>.